Received: 21 December 2022 | Revised: 21 April 2023 | Accepted: 25 April 2023

DOI: 10.1002/alz.13158

Alzheimer's & Dementia®
THE JOURNAL OF THE ALZHEIMER'S ASSOCIATION

REVIEW ARTICLE

Longitudinal amyloid and tau PET imaging in Alzheimer's disease: A systematic review of methodologies and factors affecting quantification

Ariane Bollack[1] | Hugh G. Pemberton[1,2,3] | Lyduine E. Collij[4,5] | Pawel Markiewicz[1] | David M. Cash[3,6] | Gill Farrar[2] | Frederik Barkhof[1,3,4] | on behalf on the AMYPAD consortium

[1]Department of Medical Physics and Biomedical Engineering, Centre for Medical Image Computing (CMIC), University College London, London, UK

[2]GE Healthcare, Amersham, UK

[3]UCL Queen Square Institute of Neurology, London, UK

[4]Department of Radiology and Nuclear Medicine, Amsterdam UMC, location VUmc, Amsterdam, The Netherlands

[5]Clinical Memory Research Unit, Department of Clinical Sciences, Lund University, Malmö, Sweden

[6]UK Dementia Research Institute at University College London, London, UK

Correspondence
Ariane Bollack, Centre for Medical Image Computing, University College London, London, UK.
Email: ariane.bollack.19@ucl.ac.uk

Funding information
EPSRC-funded UCL Centre for Doctoral Training in Intelligent Integrated Imaging in Healthcare (i4health), Grant/Award Number: EP/S021930/1; Department of Health's NIHR-funded Biomedical Research Centre; Innovative Medicines Initiative 2 Joint Undertaking, Grant/Award Number: 115952; European Union's Horizon 2020 research and innovation programme and EFPIA; GE HealthCare

Abstract

Deposition of amyloid and tau pathology can be quantified in vivo using positron emission tomography (PET). Accurate longitudinal measurements of accumulation from these images are critical for characterizing the start and spread of the disease. However, these measurements are challenging; precision and accuracy can be affected substantially by various sources of errors and variability. This review, supported by a systematic search of the literature, summarizes the current design and methodologies of longitudinal PET studies. Intrinsic, biological causes of variability of the Alzheimer's disease (AD) protein load over time are then detailed. Technical factors contributing to longitudinal PET measurement uncertainty are highlighted, followed by suggestions for mitigating these factors, including possible techniques that leverage shared information between serial scans. Controlling for intrinsic variability and reducing measurement uncertainty in longitudinal PET pipelines will provide more accurate and precise markers of disease evolution, improve clinical trial design, and aid therapy response monitoring.

KEYWORDS
Alzheimer's disease, amyloid, brain, longitudinal, PET, quantification, tau

1 | INTRODUCTION

The earliest pathological signs of Alzheimer's disease (AD) appear decades before the onset of symptoms.[1–3] In this preclinical stage, the primary pathological hallmarks are the accumulation of amyloid beta (Aβ) and the aggregation of neurofibrillary tau tangles, both of which can be imaged in vivo using positron emission tomography (PET). Although cerebrospinal fluid (CSF), and, more recently, plasma assays, can provide global estimates of amyloid and tau loads, molecular imaging with PET provides spatial information about the location of those protein deposits within the brain and how they change over time.[4,5] Clinical interpretation of PET images based on visual reads are simple to implement and effective in identifying marked elevations in uptake, but a further opportunity of PET comes from quantification of the AD-protein loads and their variation over time, particularly in the earliest phases of accumulation that are challenging for visual reads.[6,7]

The deposition of Aβ and tau pathologies are believed to ultimately result in neuronal death, which then leads to cognitive and functional decline. Whereas the ordering of these pathologies has largely been inferred from cross-sectional studies and can predict disease progression trends at the group level, longitudinal observations can provide more precise estimates based on individual trajectories and help determine causality. In addition, they could help uncover the substantial heterogeneity of the disease that might be overlooked when analyzing group estimates.[8] Therefore, longitudinal PET studies are valuable for improving our understanding of the start and subsequent spread of the disease and are crucial in clinical trials to assess therapeutic efficacy. In particular, the change in Aβ or tau over time has been used as secondary or exploratory endpoints in clinical trials including the ones investigating the anti-Aβ monoclonal antibodies aducanumab,[9] donanemab,[10] lecanemab,[11] and gantenerumab.[12] In addition, by determining baseline characteristics that identify individuals who are most likely to accumulate amyloid or tau, longitudinal studies can help inform enrichment strategies for trials, where improved statistical power for detecting evidence of disease modification will come from larger reductions with less variability.

To optimize the value of quantitative PET, biological and technical factors that influence the image acquisition, image reconstruction, and data analysis should be accounted for. The lack of homogeneity in processing pipelines and inherent limitations of acquisition parameters introduce uncertainties in measuring Aβ and tau protein abnormalities with sufficient precision.[13] This is well illustrated by the fact that the annual accumulation rates of Aβ and tau are on the same order of magnitude as the test–retest variability of their respective tracers.

Key factors that impact longitudinal amyloid-PET measurement uncertainty were first identified and characterized by Schmidt et al.[13] This current work aims to update the framework first proposed there. Since its publication, the number of research studies involving longitudinal amyloid and tau PET has increased substantially, allowing us to evaluate and update its recommendations. First, a systematic review of the literature to identify current strategies for measuring amyloid and tau PET accumulation over time is presented. Both amyloid and tau PET were included, as they provide complementary information about the state and spread of AD and can present unique sources of variability. We then review and update the main sources of intrinsic, biological, and longitudinal PET measurement uncertainty, emphasizing the latest techniques in areas where progress has been made. So far, most longitudinal studies rely on processing and analyzing each timepoint independently, which in turn generates independent errors. As the literature on longitudinal measures of brain atrophy using volumetric MRI has shown,[14–17] strategies that combine shared information through a joint analysis framework of all scans acquired on the same subject could reduce within-subject longitudinal measurement uncertainty.

RESEARCH IN CONTEXT

1. **Systematic review**: The authors reviewed the literature using traditional sources and meeting abstracts and presentations. The review focuses on dementia-related research studies involving longitudinal positron emission tomography (PET), and recent developments in scan acquisition, data processing, and analysis.
2. **Interpretation**: Our findings provide an overview of the current methodologies used in longitudinal PET studies. Sources of variability affecting the measure of change in amyloid and tau deposition are described, including how to address them, and which methodological features should be reported.
3. **Future directions**: The manuscript proposes a framework to help increase the precision and accuracy of longitudinal studies, with experimental designs and PET-processing pipelines specific to those studies. Examples include: (1) further investigation of sex, race, and ethnicity as sources of variability; (2) increased use of longitudinal registration pipelines; (3) guidelines defining the context of use for motion and partial volume correction; and (4) critical role of harmonization and standardization strategies.

2 | MATERIAL & METHODS

Following preferred reporting items for systematic reviews and meta-analyses (PRISMA) guidelines,[18] relevant peer-reviewed articles were identified by conducting a search on the 22/11/2021 using the PubMed database. The following query was used: ((longitudinal) OR (follow-up) OR (follow up) OR (serial)) AND ((PET) OR (Positron Emission Tomography [MeSH])) AND ((amyloid) OR (tau)) AND ((dementia) OR (Alzheimer*)) AND (brain). In conjunction, further relevant papers were searched by cross-checking pertinent references from the publications screened. No date restriction was applied to the search; only papers in English language were considered.

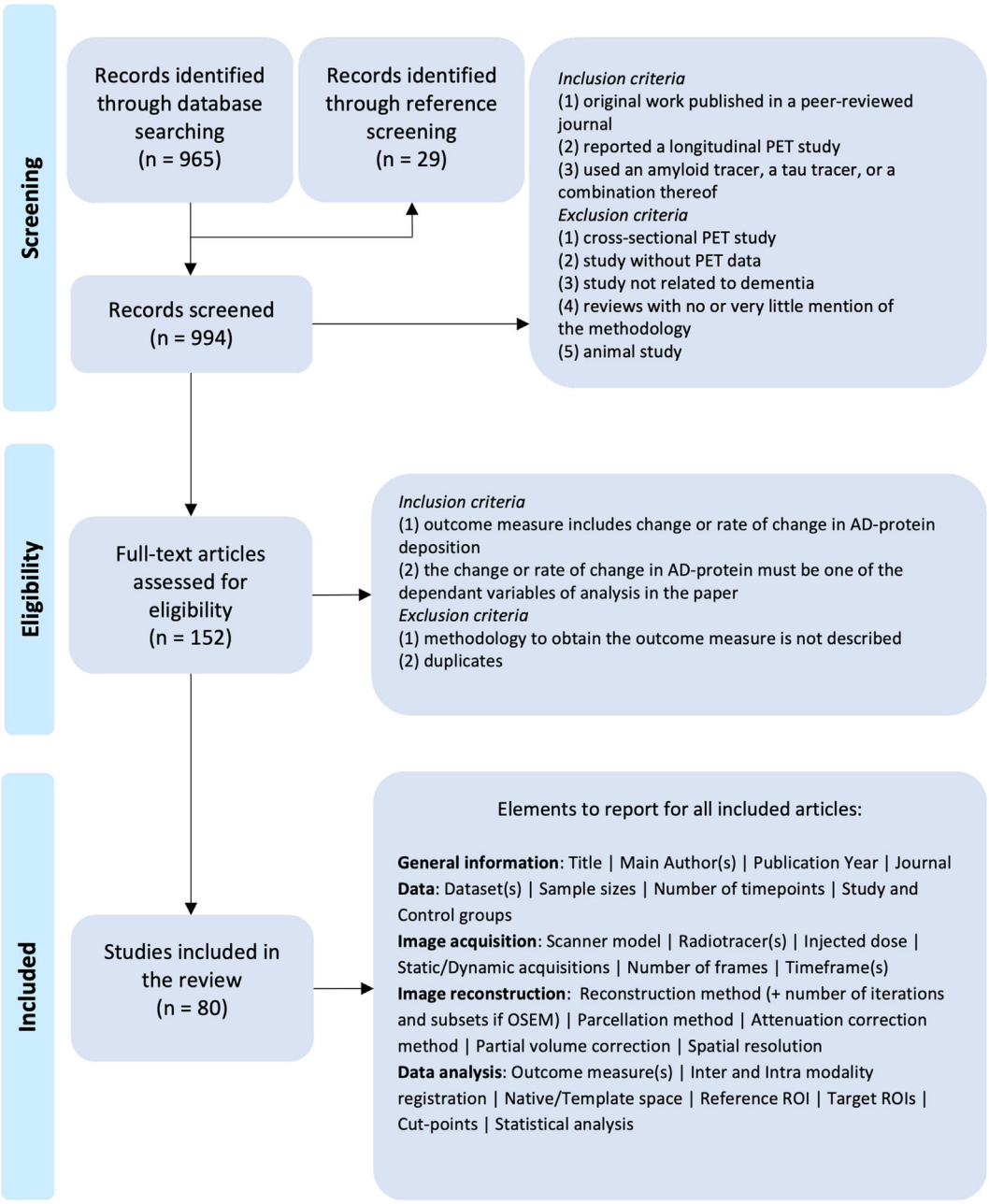

FIGURE 1 PRISMA flow diagram—PubMed search on November 22, 2021. OSEM: ordered subset expectation maximization algorithm; ROI: region of interest.

The PubMed search identified 965 candidate publications, which then went through a two-step review (Figure 1). The first step involved screening the abstracts using the following inclusion criteria: (1) consisted of original work published in a peer-reviewed journal; (2) reported a longitudinal PET study, that is, including at least one baseline and one follow-up PET scan acquired on the same individual; and (3) used an amyloid tracer (^{11}C-Pittsburg compound B (^{11}C-PiB), ^{18}F-flutemetamol, ^{18}F-florbetapir, ^{18}F-florbetaben, ^{18}F-NAV4694), a tau tracer (^{18}F-flortaucipir, ^{18}F-MK6240, ^{18}F-RO948, ^{18}F-PI2620, ^{18}F-GTP1), or a combination thereof. Exclusion criteria were as follows: (1) cross-sectional PET studies; (2) studies without PET data; (3) studies not related to dementia; (4) reviews with no or very little mention of the methodology of the articles screened; (5) animal studies.

This initial selection process yielded 152 relevant articles that were suited for further evaluation. In the second step, we reviewed the methodology and results using the following additional inclusion criteria: (1) the outcome measure involves change between timepoints or a rate of change in AD-protein deposition over time and (2) the change or rate of change in AD-protein deposition must be one of the dependant variables of analysis in the paper. Finally, we excluded: (1) articles in which the methodology used to obtain the outcome measure was not adequately described and (2) multiple papers that used identical

methodology on the same cohort to answer different questions. In the latter case, this collection of papers was treated as a single entry for the purpose of the review.

After this two-step process, 80 publications remained. In line with PRISMA guidelines, an independent researcher assessed the final selection to ensure that all included studies met the inclusion and exclusion criteria. No discrepancies were noted. For each article included in the review, we pooled data and reported several features, as described in Figure 1. The search for those features was performed screening the methodology section of each article. Supplementary material and previously published worked were also searched, when referred to in the methodology. Finally, the quality of the studies was assessed based on several factors: the research question should be clearly stated, the population sufficiently defined, the methodology adequately described and research outcomes possibly generalizable. Attention was also paid to potential selection, attrition, and reporting biases. A table listing all included publications and their key characteristics can be found in Supplementary Material.

This review is registered on PROSPERO (ID: CRD42021254695).

3 | Characteristics of longitudinal PET studies identified

Some important trends can be observed from the papers included in the review (Figure 2). First, there is a growing use of longitudinal, quantitative amyloid and tau PET, as evidenced by the rapidly increasing number of articles published since the initial framework laid out by Schmidt et al. in 2015.[13] Most longitudinal studies included in the current review used amyloid tracers (80%). This trend has started to shift with the increased availability of tau tracers allowing more studies to acquire enough longitudinal data to report findings, with tau studies representing 50% of the publications in the past 2 years. Second, more than half of the analyses have been performed on a few cohorts: the Alzheimer's Disease Neuroimaging Initiative (ADNI) and the Australian Imaging Biomarkers and Lifestyle Study of Ageing (AIBL), two valuable resources available to the global research community, as well as the Mayo Alzheimer's Disease Research Center (ADRC) and the Mayo Clinic Study of Aging (MCSA). As a result, the most common tracers used are the ones that have been selected for these studies: ^{11}C-PiB and ^{18}F-florbetapir. ^{18}F-Flortaucipir, the only regulatory approved tau tracer thus far, was used in all tau studies except one using a second-generation tracer (^{18}F-MK6240). Third, because these larger cohorts acquire longitudinal PET data on multiple cameras, processing pipelines need to account for any differences across scanners. Baseline and follow-up scans tend to be acquired on the same scanners; however, the proportion of subjects that change center or scanner in-between timepoints is rarely stated. Finally, the slow progressive build-up of amyloid plaques and tau tangles in AD led to longitudinal studies acquiring data over several years. In the selected articles, most individuals underwent PET scans around 2 years apart; however, 24% of studies reported a time interval between acquisitions of <2 years. As can be expected, most studies acquired PET scans at two timepoints (64%), although a non-negligible proportion of studies acquired more (21% studies with three timepoints, 15% with four or more timepoints).

Our literature search highlighted that many previous studies were not consistently reporting key details, which would allow the reader to properly analyze and interpret the results. Recently published PET reporting guidelines require the specification of image resolution, reconstruction, post-reconstruction filtering, attenuation correction methods, and motion correction methodology.[19] The significance and impact of those parameters on longitudinal studies and the potential importance of reporting specific technical features will be discussed further herein. In particular, reconstruction parameters were rarely reported, but could be inferred from the scanner. In the case of large cohorts such as ADNI, ADRC, or AIBL, those features can also be deduced from the main methodology papers for those studies. However, only subsets of those data sets are often used, leading to difficulties in identifying the actual technical parameters relevant to one particular study.

One of the areas where technical parameters were often not reported was image pre-processing. Motion correction was mentioned in only ≈25% of studies, of which the main technique used was frame-to-frame realignment. Furthermore, whether partial volume correction (PVC) was applied was reported in half of the studies; of those, 90% reported the specific approach implemented. The three main PVC techniques implemented were geometric transfer matrix (GTM)[20] in 48% of studies, two-compartment PVC[21] in 21% of studies, and three-compartment PVC[22] in 14% of the papers.

For studies focusing on global cortical or regional AD-protein burden, 98% of articles provided enough information about the relevant methodology for generating these regions of interest. In terms of reference regions used for standard uptake value ratio (SUVr) computations, ^{11}C-PiB studies favored the use of the cerebellar gray matter, and ^{18}F-flortaucipir more specifically the inferior cerebellar gray matter. Nearly ≈70% of studies used the whole cerebellum or the cerebellar gray matter while several publications also compared multiple reference regions. The overwhelming majority of studies relied on magnetic resonance imaging (MRI) to extract anatomic information. In that case, most commonly and when specified, the PET image is co-registered with the MRI (51%), and the analysis is then done in native PET space, native MR space, or aligned to Montreal Neurological Institute (MNI)152 atlas (35%) to ensure a consistent presentation of anatomy in a stereotactic coordinate system.

Finally, most of the reviewed articles used SUVr from static acquisitions as the main outcome measure. Although full dynamic imaging provides many benefits, there are practical limitations, even more so for longitudinal studies. This may be why some studies with dynamic acquisitions available chose to only use SUVr from the late pseudo-equilibrium frames. The Centiloid scale has started to emerge as a useful metric to provide some level of harmonization across cohorts, being used in five articles in the past 2 years—including two clinical trials.[10,23,24]

In summary, the review highlights that current studies primarily use publicly available data sets to assess change in amyloid over 2 years with static acquisitions. Image reconstruction and processing vary

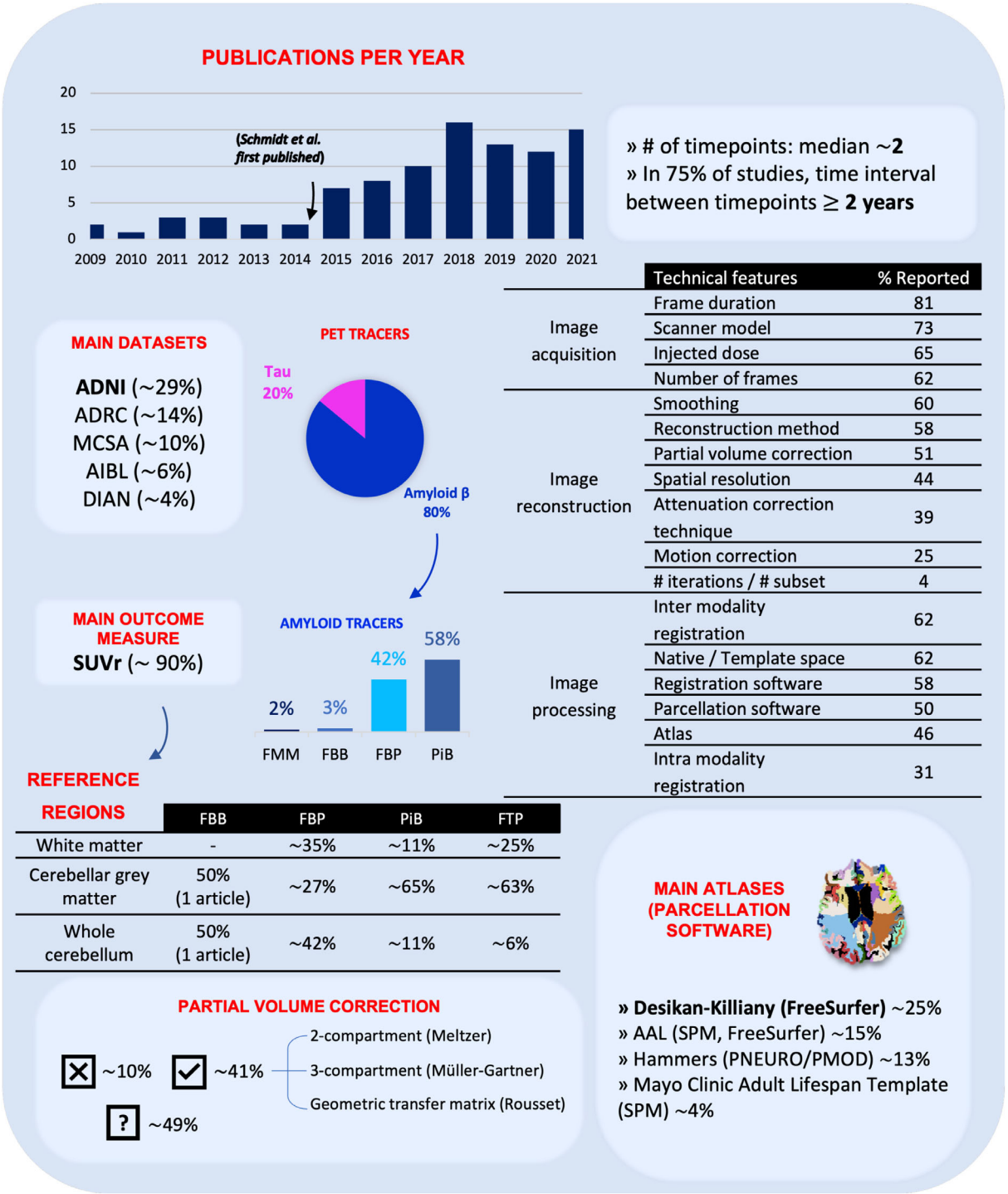

	Technical features	% Reported
Image acquisition	Frame duration	81
	Scanner model	73
	Injected dose	65
	Number of frames	62
Image reconstruction	Smoothing	60
	Reconstruction method	58
	Partial volume correction	51
	Spatial resolution	44
	Attenuation correction technique	39
	Motion correction	25
	# iterations / # subset	4
Image processing	Inter modality registration	62
	Native / Template space	62
	Registration software	58
	Parcellation software	50
	Atlas	46
	Intra modality registration	31

FIGURE 2 Overview of the literature published in peer-reviewed journals relating the use of longitudinal amyloid or tau positron emission tomography (PET) studies. Percentages represent the number of studies that report using a specific feature (radiotracer, reference region, and so on). Because some studies used multiple tracers or compared different reference regions, these percentages may not add up to 100%. ADNI: Alzheimer's Disease Neuroimaging Initiative; ADRC: Alzheimer's Disease Research Center; DIAN: Dominantly Inherited Alzheimer Network; MCSA: Mayo Clinic Study of Aging; SUVr: standard uptake value ratio; SPM: statistical parametric mapping; AAL: automated anatomic labeling; FMM: ^{18}F-flutemetamol; FBB: ^{18}F-florbetaben; FBP: ^{18}F-florbetapir; PiB: ^{11}C-PiB; FTP: ^{18}F-flortaucipir.

across studies; however, longitudinal data analyses most commonly rely on the annualized difference in SUVr, with the SUVr being computed independently at each timepoint. Although some elements of the analysis are commonly reported, several key features are omitted, making complete evaluation of the techniques difficult.

4 | Measuring change in amyloid and tau deposition

4.1 | Methodologies for computing rates of change in AD-protein deposition

Various methodologies are in use to measure the change in AD-protein deposition. The approach that requires the least amount of processing involves reconstructing and processing each scan independently. The annualized rate of change (ARC) between baseline and follow-up scans is the difference in protein load, most often in terms of SUVr, divided by the time interval between acquisitions. This rate of change can also be expressed as a percentage of change relative to the baseline value.

When more than two timepoints have been acquired, modelling the longitudinal rate of change with a linear mixed-effects model (LMM) can account for measures within each subject being highly correlated while also controlling for cofounding variables.[3,25–37] LMMs can specify random effects that characterize variability within the group level. They are also flexible, allowing variations in the number of scans and time intervals between scans. From our literature screening, we estimate that around 17% of studies used mixed-effects models; however, no clear consensus was found among the studies as to whether common covariates, such as baseline age, sex, apolipoprotein E (*APOE*) ε4 carriership, and years of education, were essential to include in models in order to sufficiently explain variability in either the uptake values at baseline or rates of change over time. As a result, depending on the nature of the sample, different models should be tested in order to determine whether these covariates explained baseline values as well as their interaction between these covariates and time.

Alternative approaches to characterize changes in PET images have been proposed that incorporate features outside of the uptake relative to a pre-specified reference region. Shokouhi and colleagues calculated Pearson correlations between regional uptake from baseline and follow-up ^{18}F-fluorodeoxyglucose (FDG) data.[38] This approach may be sensitive to changes over time, but it will not reflect whether changes represent hyper- or hypometabolism, or increased disagreement between scans. Another approach that combines information from two images into one metric is to derive a "slope" image created using a difference map.[39] Rather than focusing on magnitude of intensities within a voxel or region, the overlap index (OI) identifies the within-subject change of spatial extent of voxels with elevated tau PET signal. This approach appears to be particularly sensitive to early tau build-up.[40] Finally, one approach did not look at longitudinal changes between the two timepoints themselves, but rather in the change of a neuroimaging index based on differences in probability distribution between each image and a template of AD individuals as calculated by the Wasserstein distance.[41] The template used in the longitudinal studies was based on a leave-one-out study of 30 AD subjects from ADNI, so how well it captures the heterogeneity and subtypes within AD is not clear. Except for the OI, the ability of these methods to detect small changes compared to more standard approaches remains unexplored.

Regardless of the method used to compute the rate of change, numerous biological and technical factors influence the precision of that measure. As a result, the annual accumulation rates of Aβ and tau are on the same order of magnitude as the test–retest tracer variability. For amyloid tracers, cortical ARC ranges from <1% to 7% across studies, whereas the reported variability was 1% to 2% for ^{18}F-flutemetamol on AD subjects[42]; 4% to 9% for ^{11}C-PiB[43–45]; 3% to 6% for ^{18}F-florbetaben[45–47], and 1% to 8% for ^{18}F-florbetapir.[48–50] Variability was found to be noticeably higher for AD subjects compared to healthy controls.[44,46,49,50] Test–retest variability for tau PET was around 2%,[51] whereas ARC reported in the literature ranges from 0% to 5%.[52–54] The metric used to assess the rate of change should, therefore, always be reported with an estimation of its variability.

4.2 | Variation in longitudinal PET measurements

Variability in longitudinal PET measurements can be decomposed into three elements: (1) the true variation in protein accumulation, (2) measurement uncertainty, and (3) biologic variability.

Following van Belle's statistical guidelines,[55] we refer to uncertainty as measurement uncertainty, that is, the degree of precision with which the protein load is measured, while the term variability refers to inherent, biological heterogeneity in the longitudinal PET data. This variability cannot be reduced but can be partially accounted for in the design of PET studies (e.g., standardization strategies, subject selection) and in some cases statistical modelling. On the other hand, uncertainty can be reduced by increasing the precision of PET measurements both cross-sectionally and longitudinally. These elements will be discussed in the following sections.

5 | Intrinsic variability in protein load over time

5.1 | Genetic and demographic factors

Age, the female sex, other genetic factors (presence of the *APOE* ε4 allele, mutations in the genes encoding the presenilin 1 and 2 and amyloid precursor proteins) are established risk factors for AD. Reviews that summarise how these factors can account for inter-individual heterogeneity have been published.[13,56] These risk factors accumulate over decades to convey different levels of risk. In a longitudinal study, the patient serves as their own control and quite often these confounds have far more impact explaining variability at baseline than on measured rates of change in protein deposition over a typical 2-year interval.

Although *APOE* is the largest genetic risk factor for sporadic AD, it is important to note that the level of risk conveyed by carrying an

ε4 allele has been shown to vary by race and ethnicity. ε4 carriership increases risk of developing AD for White individuals but not significantly for African Americans and Hispanics.[57,58] Several studies have assessed the impact of *APOE* ε4 carriership on the rate of AD-protein accumulation, with differing results. Some studies found that fibrillar amyloid accumulates at greater rates in *APOE* ε4 carriers than in noncarriers[34]; some indicate that this difference occurs only during early stages of the disease[32,59]; and others reported that carriership is not related to the rate of change but rather the age at onset.[31,60] Key elements to consider are that *APOE* ε4 carriers are more likely to accumulate Aβ pathology versus non-carriers, and importantly tend to develop the disease earlier,[34,61] which could explain higher rates of Aβ accumulation for *APOE* ε4 carriers in study groups with lower amyloid burden.[31,59] A gene dose-dependent effect has also been suggested.[62] Moreover, an *APOE* effect was also found for tau accumulation, with accumulation possibly being more prominent in ε4 carriers.[63] Finally, the ε2 allele might have a mild protective role by slowing down amyloid accumulation.[27,32]

The female sex is another well-recognized risk factor,[64] although the influence of sex on longitudinal PET biomarkers has been relatively little studied.[65] In contrast to amyloid, emerging studies focusing on tau suggest diverging courses of protein deposition over time. For instance, Smith et al. found a higher rate of tau accumulation in females compared to males.[66] For cognitively normal individuals with high amyloid load, it has also been shown that females exhibited higher tau load in the entorhinal cortex compared to men.[65] Further studies will be needed to confirm those observations and better understand the factors driving those differences.

Race and ethnicity are being investigated as additional causes of biological variability. In a single-site cohort from Washington University in St. Louis, there was no evidence of a cross-sectional difference in neocortical SUVr (as measured by ^{11}C-PiB or ^{18}F-florbetapir) between African American and non-Hispanic White subjects.[67] On the other hand, results from the multi-site A4 and IDEAS study suggest decreased rates of amyloid positivity and/or decreased SUVr in Asians, Hispanics, and Black participants who met the eligibility criteria for these studies.[68–70] Results on the effects of race and ethnicity on tau PET uptake are also mixed. An additional analysis of the cohort in Morris et al.[67] showed no evidence of a difference in flortaucipir PET uptake based on race.[71] However, Black/African Americans had elevated ^{18}F-flortaucipir PET binding in the choroid plexus (with a possible spill-in effect onto the hippocampus),[72] bilateral occipital, temporal, and superior frontal areas[73] compared to White individuals. This could be linked to non-specific binding of ^{18}F-flortaucipir to melatonin in the meninges, which is found in higher quantities in darker skin types.[74] Further studies should be performed because differences in assessed tau load due to non-specific binding or other physiological issues could impact the definition of positivity thresholds. Although non-Hispanic White individuals are over-represented in longitudinal AD studies, including clinical trials,[75] investigating whether there is an impact of race and ethnicity on the rate of protein accumulation will improve our understanding of differing risk factors for AD and more comprehensively characterize the underlying AD pathology.[76]

Overall, although these demographic and genetic factors increase the risk of developing AD, it is not clear whether this risk is conferred through increased rates of accumulation in AD pathology or if similar levels of pathology result in earlier onset.

5.2 | Disease subtypes and staging models

AD is not a monolithic entity but is characterized by substantial heterogeneity with a spectrum of typical and atypical clinical presentations, with varying ages at onset and rates of disease progression.[36,77–79] Identifying subtypes can help uncover group patterns that better characterize the heterogeneity of the disease. Multiple classification schemes have been developed to reflect AD variants based on heterogeneous clinical presentations and imaging patterns. For instance, quantification on a regional level and beyond dichotomization of amyloid and tau status to positive and negative could help predict inter-individual as well as group trajectories. Longitudinal data can be useful to build[80–82] and validate amyloid[83] and tau progression models.[84–86] These various patterns of protein deposition are not fully understood and could be linked to specific genetic susceptibility.[86]

5.3 | Blood flow

Variability in cerebral blood flow (CBF) directly influences tracer delivery and clearance,[87,88] and can, therefore, add uncertainty, particularly to measures from static acquisitions where it is assumed a pseudo-equilibrium has been reached.[89–91]

Longitudinal studies might be particularly impacted by the presence of CBF changes over time,[91] which may occur with increasing age, disease progression, and therapeutic interventions.[92] A simulation study by Ottoy et al. suggested that reduced CBF is expected in subjects with mild cognitive impairment (MCI) and AD patients, in particular in the posterior cingulate, which agrees with previous results by Cselényi et al.[93,94] These simulations were based on fully dynamic ^{18}F-florbetapir data and showed that changes in relative CBF can produce apparent changes in SUVr in patients with AD, increasing with the disease severity. This was also observed on ^{18}F-florbetaben data.[89]

Blood-flow alterations can be accounted for through kinetic modelling of dynamic acquisitions to derive non-displaceable binding potential (BP_{ND}) or distribution volume ratio (DVR = BP_{ND} +1). Heeman et al. compared methodologies to obtain DVR from ^{18}F-flutemetamol and ^{18}F-florbetaben PET data and found that reference Logan quantification was more robust to changes in blood flow than the simplified reference tissue model (SRTM).[95] These findings are in line with similar ^{11}C-PiB studies.[96] Furthermore, the impact of blood flow on SUVr measurements has been shown to be more dependent on the reference region than the target, as CBF changes in the white matter (WM) will have more effect than when the cerebellum is used as the reference.[89,93]

Finally, Cselényi et al. extracted a blood-flow component in cortical SUVr and found significant negative relationship between R_1

representing the ratio of tracer delivery and SUVr (≈0.04 unit increase in SUVr for every 0.1 unit decrease in R_1 at a constant DVR).[94] The R_1 has demonstrated low test–retest variability over time (≈1.70% for a global composite region), which might make it particularly suitable as a surrogate measure of CBF in longitudinal studies.[91,97] Overall, SUVr from ^{18}F-flutemetamol and ^{18}F-florbetaben data tend to overestimate protein binding via DVR, which should more closely reflect ground truth, with this effect being proportional to the Aβ load.[98] This overestimation was also observed in a ^{18}F-THK-5351 tau PET study.[99] Longitudinal studies with individuals that are cognitively impaired or have higher amyloid burden could be particularly affected by this bias, leading to an under- or overestimation of their rate of amyloid accumulation. Despite the challenges of implementing longitudinal, dynamic PET studies, 13% of articles in the reviewed literature used dynamic acquisitions.

6 | Reducing PET measurement uncertainty

6.1 | Scan acquisition factors

Subject motion

Head motion can degrade the image quality and subsequently the accuracy of protein quantification. For instance, simulating realistic motion, Chen et al. found an ≈4% relative change between corrected and non-corrected FDG data.[100] Regional and voxel-wise analyses, particularly relevant to study tau spreading over time, can be impacted severely by motion-related errors as regions that are smaller, more lateralized with a high degree of curvature (such as the lateral orbital frontal cortex) are more likely to be misquantified.[100]

Motion can occur between the attenuation correction scan and the PET acquisition leading to emission-attenuation mismatch between timeframes and within (averaged) PET timeframes, as detailed previously by Schmidt et al.[13] To help address the first two, in the case of a PET-CT (computerized tomography) acquisition, the amyloid PET Quantitative Imaging Biomarkers Alliance (QIBA) profile recommends co-registering the PET frames to the CT image prior to attenuation and scatter corrections, and if not feasible, to remove frames or whole scan when motion exceeds 4 mm or 4 degrees.[101] Motion correction is still an active area of research, with recent developments following progresses in optical tracking and neural nets.[102,103] Within-frame motion remains the most challenging to detect and, therefore, correct; however, novel techniques relying on multiple reconstructions from very short PET frames have been developed that can address this issue.[104] The full range of motion-correction techniques is beyond the scope of this review, but are summarized elsewhere.[105]

Studies focusing on when to perform motion correction could be valuable, as mis-registration and interpolation (particularly when motion is minimal), can also introduce inaccuracies in the final PET measure.[106,107] In addition, serial PET measurements will likely be highly affected by motion, as differing types and magnitudes of motion across timepoints could lead to an under- or overestimation in rates of change computations, even more so in regional analyses. Although motion correction has a significant impact on the accuracy of the final metric, most often the use of such techniques is not reported (in 25% of articles screened), contrary to the latest PET-reporting guidelines.[108]

Duration of acquisition

The duration of the acquisition can influence the accuracy of the PET measure. A continuous, dynamic acquisition from tracer injection to pseudo-equilibrium allows quantification of tracer uptake with standard kinetic-modelling techniques. As mentioned previously, this approach is more accurate than SUVr, since kinetic modelling can account for the effects of blood flow. On the other hand, SUVr derived from static acquisition reduces cost and burden to the patient due to the shorter acquisition time required. Motion is also likely to be reduced during these shorter acquisition periods.

Given that the kinetics of some tracers require nearly 2 hours from injection to reach pseudo-equilibrium, dual time-window protocols have recently been proposed to allow kinetic modelling while reducing the total acquisition time. A patient is first scanned during tracer injection and wash-in, and then a second time when the tracer has likely reached pseudo-equilibrium. Kinetic modelling is then performed by combining the two sections of the time-activity curve using interpolation to fill the region of the curve in between the two acquisitions. An optimized dual-time window for amyloid tracers ^{18}F-florbetaben and ^{18}F-flutemetamol, which was designed to minimize the bias and the number of outliers, was 0-30 min post injection (p.i.) and 90-110 min p.i.[109] Bullich et al. reported similar timings (0-30 and 120-140 min p.i.).

Dual time window acquisitions have also been investigated for tau tracers. Protocols similar to the ones described previously herein have also been implemented for ^{18}F-flortaucipir (0-30 min p.i. and 80-100 min),[110] with one caveat for ^{18}F-flortaucipir being that many studies suggest that the tracer uptake does not reach a plateau but continually increases after the time of injection until the end of acquisition.[111,112] A dual time-window strategy was also achievable for ^{18}F-MK-6240, with the acquisition phases being 0-30 min p.i. and 90-120 min.[113] Kolinger et al. noted that the dual-phase protocol might be less robust to blood-flow variations than a full dynamic acquisition. In order to limit inter- and intra-individual variability arising from variations in time windows, a time correction was implemented by Pontecorvo et al.[53] For each voxel, a linear regression is fitted through all available PET time frames to create adjusted images representing a consistent post-injection time window.

Dual time-window protocols might be beneficial to implement in longitudinal studies, as reducing the total acquisition time required to obtain suitable data for kinetic modelling may lead to more accurate quantification by accounting for confounds such as tracer delivery compared to SUVr approaches, while the shorter acquisition time should decrease the level of motion.

Long axial field of view PET scanners

Current PET scanners have an axial field of view (FoV) of ≈20 cm, which can cause lower parts of the brain to be cropped or to be noisy due to their proximity to the edge of the FoV. This is especially important as the cerebellum is very often used as a reference region, which can lead to an overestimation of the SUVr, as noted by Schmidt et al.[13] In longitudinal studies, differences in the positioning of the subject within the FoV at different timepoints can bias the estimate of change in protein load.

This can be addressed by acquiring data on long axial FoV scanners,[114] such as the two first total body PET-CT scanners, the EXPLORER (United Imaging Healthcare Co, Shanghai, China)[115] and the Biograph Vision Quadra (Siemens Healthineers, Knoxville, TN, USA),[116] with axial FoV of 194 and 106 cm, respectively. These scanners present new potential opportunities: increased signal-to-noise ratio, shorter scanning time (reducing the risk of motion), reduction in dose, increased temporal resolution, and ability to derive a true image-based arterial input function from the aorta.[116–118] Although more sensitive PET scanners could be particularly advantageous for longitudinal studies, they might not be well suited for claustrophobic patients, and their high cost might be a major limitation to their widespread use, especially for AD-related brain imaging.

Dose-reduction strategies

Dose-reduction strategies could be relevant for longitudinal studies, and worth investigating if PET is to be used more frequently to monitor disease progression and effects of treatment. These strategies are promising and provide clear benefits to patients. Apart from a reduced risk for patients, it could also allow more detailed investigations of differences between tracers if the dose is sufficiently reduced to stay within radioactive substance regulations. Although dose-reduction strategies have been implemented for FDG,[119,120] fewer studies exist for amyloid and tau PET acquisitions. Nai et al. showed that reconstructing images from low-count PET images using ^{18}F-THK5351 and ^{11}C-PiB data introduces varying degrees of bias depending on the processing pipeline. The DVR resulted in the best quantitative accuracy, with <7% bias across regions.[121] An ultra-low-dose strategy has been developed by Chen et al., which uses a deep learning approach to synthesize PET images from multiple MR sequences and a low-count PET image.[122] Long axial FoV scanners discussed previously could lead to lower dose requirements, although the impact on quantification beyond visual read should be evaluated. In longitudinal settings, dose-reduction strategies may allow more frequent PET acquisitions; however, distinguishing noise from the actual variation in Aβ or tau with an additional measurement bias and a shorter time interval in-between scans might not be feasible at this time.

6.2 | Image reconstruction factors

Partial volume effect

Partial volume effect (PVE) is one of the main physical factors limiting the quantitative accuracy of PET. It can be seen as the combination of two effects. First, due to the discrete sampling, a single voxel in the reconstructed image can contain a mixture of tissues with different levels of uptake (gray matter, white matter [WM], dura, meninges, cerebrospinal fluid [CSF]). Second, the relatively poor PET spatial resolution (≈3 mm to ≈7–8 mm depending on the scanner), modelled via the point spread function, causes spill-out/spill-in of one region onto another. In longitudinal studies, PET quantification can particularly be affected by PVE for subjects with brain atrophy.[123] Compared to amyloid, tau studies are more likely to require regional protein estimates and study individuals with more advanced AD and atrophy. They are, therefore, especially prone to PVE quantification errors. The adoption of PVC in routine image processing has been limited so far (41% of our selected publications). Importantly, these methodologies require an accurate specification of the point spread function model and the precise co-registration of PET and MR, as small misalignments can cause PVC methods to add noise rather than reducing it.[106,107]

Most studies found that PVC increases the change in tracer uptake but also increases the measurement uncertainty.[5,124–127] Increases in rates of change due to PVC may affect subjects with higher amyloid more, as suggested by Brendel et al. who found a decrease in percentage change over time in healthy controls and MCI subjects, versus an increase in AD subjects.[125] Such differences were also observed by Rullman et al., who found a significant effect of PVC on Aβ-positive subjects, but none on Aβ-negative subjects,[126] and a significant positive effect of PVC in MCI and AD groups in another study.[127] These results suggest that atrophy-related PVE occurs at a higher rate in MCI/AD subjects, could mask the true PET signal increase, and could, to some extent, be recovered by PVC.

On the other hand, some studies found no apparent effect of PVC on the rate of change of protein deposition for ^{18}F-flortaucipir scans[128,129] and ^{11}C-PiB.[2,130] The difference in findings could be attributed to shorter time intervals in-between PET acquisitions, making it more difficult to detect PVC-related changes.

Finally, the choice of PVC implementation can have a substantial effect on variability. The most commonly used techniques in longitudinal PET studies include the two-compartment model or Meltzer method,[21] the three-compartment or Müller-Gärtner method,[22] and the geometric transfer matrix (GTM) by Rousset et al.[20] Some studies used the region-based voxel-wise (RBV) correction[123] and iterative Yang technique.[131] Schwarz et al. evaluated the performance of the former three techniques longitudinally. Although GTM was the most used technique in our literature screening, it was found to have less relative precision assessed by the residuals from mixed-effects models compared to Meltzer and Müller-Gärtner style PVC (longitudinal variability of ≈4% to 8% compared to ≈2% for traditional methods).[132]

The GTM method seems to offer better group separation between impaired and unimpaired individuals, but it suffers from larger levels of uncertainty.

Although PVC was reported in only 40% of the articles in his review, the findings support a wider use of PVC for longitudinal studies, especially for individuals with brain atrophy—provided some quality control is in place to ensure an accurate PET/MR registration when MR is used. In reviewing the relevant literature, GTM was the most common PVC technique implemented in nearly half of the studies using PVC; however, traditional two-compartment and three-compartment PVC seemed to provide more stable estimates of amyloid accumulation and might, therefore, be preferable to GTM. Further studies comparing the precision, accuracy, and robustness of these PVC techniques in longitudinal settings are warranted.

Attenuation correction

The accurate quantification of the PET signal is heavily dependent on the accuracy of the attenuation correction. The original attenuation correction methods relied on a PET transmission scan using Germanium-68. With the advent of PET-CT systems, a low-dose CT was acquired to generate an attenuation coefficient map by converting Hounsfield units into linear attenuation coefficient via a piecewise linear transformation.[133] PET-MR presents different challenges for attenuation correction, as standard MR-imaging techniques cannot provide an accurate estimate of an object's electron density, leading to difficulties distinguishing bone from air and other tissues, and the smaller bore and strong magnetic field do not allow for a PET transmission scan to be performed. MR-based attenuation-correction sequences are available for the two currently available PET-MR scanners: the Biograph mMR (Siemens Healthcare GmbH, Erlangen, Germany) and the Signa PET/MRI (GE Healthcare, Waukesha WI, USA). However, several alternative methods have been proposed to improve the accuracy of attenuation correction for PET/MR systems.[134]

Attenuation correction technique was reported in 39% of the reviewed studies: 31% based on CT and 60% on transmission scans. No MR-based methodologies were mentioned specifically, although it is probable that the default attenuation correction from the scanner manufacturer was used in those cases.

Regardless of the methodology, the accuracy of the attenuation correction strongly depends on an accurate estimation of the attenuation-correction map and co-registration to the PET scan, with any misalignment likely due to subject motion.[135] Chen et al. simulated misalignment, and estimated a bias in SUVr of 2.5%, 4%, and up to 10% in respectively low, moderate, and large motion models.[100] Any motion-induced cross-sectional uncertainty could have an even higher impact for longitudinal imaging, although to the best of our knowledge, no study on that topic has been conducted. An accurate registration of the μ-map to the PET scan or the implementation of a motion correction algorithm could be used to address this issue.

6.3 | Image processing and analysis factors

Reference region

Even in fully dynamic acquisitions, kinetic modelling using arterial blood sampling is rarely used, thus a reference region consisting of tissue with minimal uptake needs to be defined. The reference region chosen to normalize tracer uptake is one of the most common sources of variability between scans. It is influenced by many factors, including the choice of tracer, the scanner's axial FoV, the precision of the alignment with the images defining the regions of interest (ROIs), the quality of the parcellation, atrophy, and its sensitivity to variations in blood flow.[95] Overall, the choice of reference region is still a subject of debate and varies with the context of the study. The interpretation of SUVr values will also have to be adapted to the reference region used, as the resulting values have different ranges (see Figure 3).

The most common reference regions used in the literature are the whole cerebellum, the cerebellar gray matter, the pons, the brainstem, the (eroded) supratentorial white matter (sWM), and a composite reference typically combining some or all of these regions.[48] Due to non-specific uptake near the falx cerebri, tau tracers often further restrict the reference region to inferior regions of cerebellar gray matter.

Several studies suggested the use of the sWM as a suitable reference region for longitudinal studies.[33,48,124,125,136,137] This finding could be due to this reference region being large and more contiguous, and, therefore, less susceptible to noise, PVE, and registration errors. In addition, compared to the more widely used cerebellar and pontine reference regions, the sWM might be less sensitive to differences in the patient's head positioning within the FoV across several timepoints, whereas SUVr normalized to the cerebellum can be overestimated in cases where the cerebellum is cropped or near the edge of the image due to small axial FoV in some scanners.[48,137]

As a result, compared to other reference regions, SUVr computed using sWM showed significantly less variability over time and greater power to detect change in protein deposition, as well as less implausible negative trends over time in studies acquired with ^{18}F-florbetapir,[48,124,125,136,137] ^{11}C-PiB,[33,138] and ^{18}F-flortaucipir.[54,139] An alternative approach for ^{18}F-flortaucipir using a subject-specific WM reference region based on the Parametric Estimation of Reference Signal Intensity (PERSI) was also found to be more reproducible and stable over time than other common reference regions,[139] resulting in a tau metric more sensitive to change.

Despite these benefits favoring the use of the sWM over other reference regions, several concerns have been raised both for amyloid and tau regarding the stability of the sWM over time. The sWM uptake has been shown to increase with age as well as cortical amyloid load,[33,140] and the pharmacokinetic properties of sWM differ from the gray matter. A ^{18}F-florbetapir study showed that sWM is more susceptible to blood-flow alterations than the cerebellum,[140] and suggests that the stability of the sWM over time is mainly due to lower statistical noise compared to the cerebellum. Regarding ^{18}F-florbetaben,

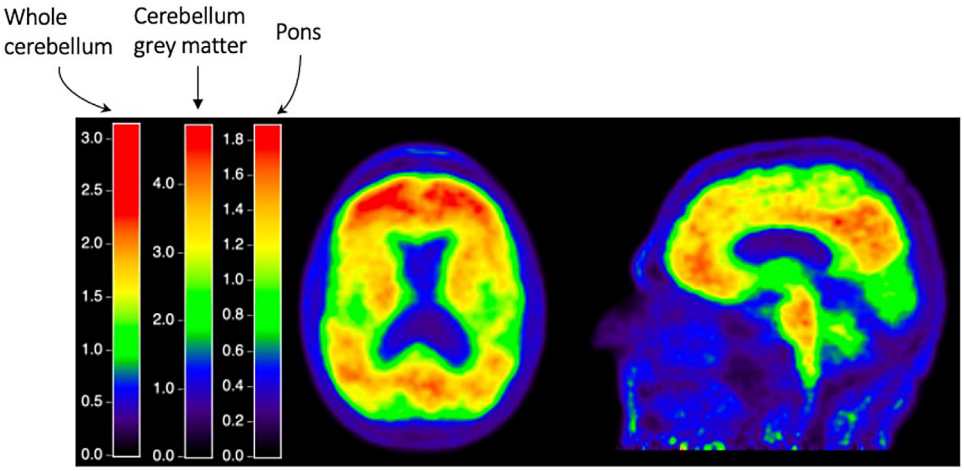

FIGURE 3 Example of an SUVr parametric map obtained from a ^{18}F-flutemetamol PET scan. The color bars illustrate the different ranges of SUVr depending on the choice of reference region.

studies showed that the sWM had low sensitivity to differentiate between Aβ-positive and Aβ-negative individuals and was less stable over time than the cerebellar gray matter.[141,142] Moreover, in longitudinal studies, sWM quantification might also be impacted by changes in WM integrity, further increasing the variability of the SUVr. Reduced amyloid uptake has been linked to WM hyperintensities[143]; however, a review paper from 2017 aggregating results from 34 studies suggests that there is no direct association between the two.[144] Regarding tau, a study by Moscoso et al. demonstrated a decreased retention of ^{18}F-flortaucipir in regions with WM hyperintensities, and that up to 57% of the variance in longitudinal SUVr linked to variations in the reference region tau uptake.[145]

Finally, the use of WM as reference region is not recommended for conversion to the Centiloid scale (CL) as it was shown to add significant measurement variability compared to cerebellar-based reference regions[146] and could lead to underestimation of the amyloid load.[147]

Novel methodologies have been created to address issues caused by dependency on anatomically defined reference regions: the evaluation of brain amyloidosis (ELBA),[148] the Aβ-PET pathology accumulation index (Aβ index),[149] AMY Q,[148,150] and the amyloid pattern similarity score (AMPSS).[151] These methods are independent of a reference region and are described in more detail later. Although these data-driven approaches show promising results, the advantage of the SUVr lies in its simplicity and therefore wide usage across studies with static acquisitions.

Regions of interest

Identifying an appropriate target region will also impact the performance of longitudinal analyses. Common choices are to use a global neocortical ROI, selecting individually defined anatomic regions that have been identified as being particularly vulnerable to AD pathology or composite regions designed to capture a summary of AD-related changes. On one hand, global regions will likely be more robust to noise and measurement error than smaller individual regions; however, they may combine areas of high change and low change together, reducing the ability to detect changes in the early phases of the disease. Creating a composite region attempts to find the balance between the two—more sensitive than a global measure but less susceptible to error than an individual region. For amyloid tracers, the composite region often comprises the frontal, anterior/posterior cingulate, lateral parietal, and lateral temporal regions.[48] The regions commonly used in tau imaging tend to be grouped according to Braak staging[152,153]: amygdala, entorhinal cortex, fusiform, parahippocampal, and inferior temporal and middle temporal gyri. Due to spill-out effects from non-specific binding in the choroid plexus, accurately quantifying tau binding in the hippocampus using ^{18}F-flortaucipir can be challenging,[154,155] but it may be mitigated with effective application of PVC.[156] Longitudinal trajectories at the regional level for amyloid[157,63,125,62,158,36,159] and tau[5,77,86,54] have been investigated but are beyond the scope of this review.

Various atlases have been employed for the definition of the target region, and the corresponding labelling protocols for key structures may vary from atlas to atlas. In the studies included in this review, five atlases were commonly used: the Desikan-Killiany atlas,[160] implemented in FreeSurfer in 25% of studies[31,63]; the Automated Anatomical Labeling atlas,[161] in around 15% of studies[27,35]; the Hammers atlas,[162] available in PNEURO/PMOD, in around 13% of studies[36,59,124,125,163,164]; the Mayo Clinic Adult Lifespan Template (MCALT) atlas, in 4% of studies[77,129,165]; and the Harvard-Oxford atlas (2%).[83,166] Neuroparc, a standardization method across brain atlases has been developed recently,[167] and could help with comparing data obtained with different atlases.

Apart from the choice of reference and target regions, the accurate co-registration between PET and atlas is critical to the precision of longitudinal PET measurements. Even in PET-MR scanners, motion can introduce a misalignment between the atlas derived from the MR and the PET data. According to Schwartz et al., who quantified the impact of this misalignment, motion accounts for ≈1% of the test–retest

variability of amyloid PET, which in turn results in a rate of change with a variability of ≈7%.[107] The choice of registration software is also crucial as shown by Markiewicz et al., who compared four common registration softwares and found that Statistical Parametric Mapping (SPM, Wellcome Trust Centre for Neuroimaging, London, UK)[168] resulted in the lowest measurement uncertainty.

Novel "data-driven" metrics of amyloid and tau deposition

The more established protein deposition metrics—including SUVr, BP_{ND}, the CL—all present limitations. Although SUVr is simple to compute and can be derived from a short static acquisition, it is dependent on many factors (e.g., choice of reference region [see Figure 3]; length of the FoV; quality of the parcellation; precision of the alignment between the MR, the CT, or the atlas; stability of that region over time; variations in blood flow). The BP_{ND} is a more accurate measure of the density of available receptors as it considers the effect of blood flow, but it requires long, dynamic acquisitions that cannot be implemented easily in a clinical setting or standardized across multiple centers. CL offers an opportunity to harmonize SUVr-based metrics, using post hoc linear transformations to a scale calibrated by a reference ^{11}C-PIB-based SUVr data set. The SUVr remains the most established metric, whereas the use of Centiloid has steadily increased since its development in 2015 and is now used in many studies including clinical trials.[10,23] Nonetheless, several studies drew attention to the robustness of this metric when different tracers are used, which could be particularly relevant in a longitudinal setting.[169–172] These limitations as well as the increased number of longitudinal PET studies (see Figure 2) triggered the development of novel, alternatives methods to quantify the protein load.

Data-driven PET analysis methods rely on the assumption of a multivariate pattern of amyloid deposition that can be captured across the population. Several metrics use image decomposition to extract the specific tracer binding. The amyloid load ($A\beta_L$) and tau load (Tau_L) by Whittington and Gunn describe the SUVr trajectory over time using a logistic growth model, assuming that each brain region has a maximum capacity to carry amyloid.[52,173,174] Many methods use dimensionality reduction techniques such as principal component analysis (PCA)[149,150] or non-negative matrix factorization (CL_{NMF})[169] to compactly represent this multivariate pattern, often optimizing the weighting of the largest component to create an adaptive template to obtain more accurate registrations.[149,175] Further improvements have explored how to make these methods more robust to different tracers[169] and not require a reference region.[149,150] Also based on image decomposition, the specific Aβ load (SAβL) uses deep learning to generate a map of non-specific binding from MR sequences. This map is then subtracted from the original SUVr image to obtain a map of specific binding.[176,177] The ELBA takes a very different approach and tries to translate visual interpretation of images mathematically. It does so by capturing the variation in the image intensity using two criteria: a metric of iso-intensity surface complexity and one that evaluates the histogram propensity toward higher values. These metrics are optimized and combined to form the ELBA.[148]

Among all these methods, the $A\beta_L$, Tau_L, ELBA and CL_{NMF} have been evaluated against longitudinal data. The $A\beta_L$ showed increased sensitivity assessed by the effect size of the change in amyloid burden (Hedges g = 0.49 compared to 0.36 for SUVr) and increased ability to separate scans between clinical groups. Another study using AβL also found lower longitudinal variability in AβL compared to SUVr, but only for amyloid-negative subjects.[178] The equivalent approach for tau tracers, Tau_L, showed greater effect size than SUVr for the change in tau deposits between six clinical groups, which suggested that smaller sample sizes would be required to show a 25% reduction in tau accumulation over 1 year (power = 80%, $\alpha = 0.05$). The longitudinal consistency was assessed for ELBA by using the standard deviation of the residuals from least square linear regression with respect to time between scans. The ELBA technique performed better than SUVr, with a variability normalized by the interquartile range of ±2.3%. Finally, compared to CL, the CL_{NMF} was shown to have greater longitudinal consistency with fewer abnormal changes over time, to be more robust to change in tracer between timepoints, and to have a stronger association with baseline value (Spearman ρ of 0.39 vs 0.21 for CL). Although promising, these novel metrics should be evaluated further in longitudinal settings.

6.4 | Toward simultaneous image reconstruction, joint PET image processing, and analysis

The most common approach to analyzing longitudinal PET data is to obtain outcome measures from each timepoint independently. This is a practical solution, particularly if different timepoints have been acquired on different scanners. However, images acquired from the same subject represent repeated measures, which contain large amounts of shared information that could increase the precision of longitudinal protein change by reducing the (differential) image noise. This advantage has been clearly demonstrated in research on structural MRI.[14,16,179] There are many points within the reconstruction and pre-processing pipeline where this shared information may be leveraged.

Joint image reconstruction

Ideally, the optimal place to incorporate shared information would be the earliest point of analysis, during the image reconstruction. Ellis and Reader[180] developed a joint reconstruction method for two images that incorporate priors based on shared characteristics of the images.[181,182] Joint reconstruction was also implemented in a framework using linear temporal dependency and spatial alignment between scans to build a difference image with greater contrast, which resulted in reduced sample sizes to detect change in SUVr.[183] These methodologies have been tested primarily for a situation with two scans; the feasibility of these approaches with multiple scans remains unclear.

FIGURE 4 Overview of registration strategies used in longitudinal PET pipelines.

PET-MR pipeline

- PET registered to MR which is then warped into MNI space
- PET registered MR followed by the analysis in the native MR space
- MR registered to PET, followed by a native PET analysis using MR parcellations
- Longitudinal registration pipeline with mid-point space
- Follow up PET-MR registered to baseline PET-MR

PET-only pipeline

- Registration of atlases into PET space using specifically designed PET templates corresponding to tracer and amyloid status
- Registering PET into MNI space using specific PET templates
- Follow up PET registered to baseline PET

Implementation within a clinical setting could be challenging due to the increased storage and computational requirements of retaining raw list mode data from all timepoints, as this format of the data needs orders of magnitude more storage than the resulting reconstructed images.

Joint image processing

Besides reconstruction, there are still other steps later in the processing stage where shared information can be leveraged. Defining a common space for image analysis is particularly relevant in the case of longitudinal studies where two or more scans are compared at the individual level. Here we focus on registration strategies in two contexts: PET-only pipelines and PET-MR or PET-CT pipelines. The most common registration strategies from the reviewed literature are described in Figure 4.

The final analysis space varies between studies; the most used ones are the native PET and native MR space, as well as a standard (usually MNI) space. Many studies opt for MNI space to normalize their data and help compare scans both at the individual and at the group level. However, Kolinger et al. compared the impact of the reference space for analysis on the SUVr and found no significant difference between native and standard space, but any image feature using volumetric information should be performed in native space.[184]

With the increasing availability of longitudinal registration pipelines for structural MRI, a few studies have begun to implement them into longitudinal analysis of amyloid and tau PET data.[26,39,54,66,185] Longitudinal registration pipelines are available in SPM,[179] FreeSurfer,[16] and ANTs.[186] These pipelines create unbiased, within-subject templates that tend to be equidistant from each timepoint included in the registration. In short, PET images are first rigidly registered to the MR closest to it in time. The serial MR scans are then co-registered to form the within-subject template. Next, the parcellation can be derived from the within-subject template or the parcellations are first obtained in native MR space and transformed into the midpoint space. By overlapping the parcellations from all timepoints, the final selection of ROIs can be cropped to include only voxels belonging to all timepoints. This more conservative approach of excluding voxels within a region could be particularly useful when substantial atrophy over the course of the study is likely.[185]

Using these longitudinal techniques from high-resolution MRI could improve the precision of longitudinal PET measurements by reducing the noise introduced by distinct processing pipelines, as well as reducing potential sources of bias. Early longitudinal pipelines of structural MR, which transferred follow-up scans onto the baseline for analysis, have been shown to cause a bias arising from the asymmetry of transformations and subsequent resamplings applied to the follow-up scans in comparison to the baseline.[187,188] Although evaluation of longitudinal pipelines has focused predominantly inwards around accurately measuring change in various structural metrics of neurodegeneration, initial evaluations to the impact of PET have begun. Both the MR study of Tustison et al. and the tau PET study by Schwartz et al. found that longitudinal pipelines were able to produce more stable measures of change over time and increase cognitive group separation[186,189]; however, what elements of longitudinal pipelines have the most impact on improving precision requires further work.

Further approaches that use all of the timepoints to produce longitudinally consistent outcomes should be examined. For instance, besides generating a consistent parcellation, the longitudinal registration pipeline could be applied to generate a shared attenuation correction map, independently of which modality it is derived from, or use the same one for both timepoints. Future studies could also investigate incorporating shared information to dynamic acquisitions, for instance by performing a joint kinetic modelling of all timepoints.

7 | DISCUSSION

In this review we present an overview of the state-of-the-art of longitudinal amyloid and tau PET studies. In summary, technical factors such as motion, registration strategy, PVE, and the choice of reference region are the biggest sources of variability in longitudinal PET measurements. First, motion correction should be more commonly implemented using robust and accurate registration techniques, as it has been shown to lead to up to 7% imprecision in the measure of change in SUVr. Next, many studies suggest that PVC should be used, especially in the case of longitudinal tau studies, where spill-in from off-target binding and substantial evidence of correlation between tau deposition and atrophy patterns could introduce errors in measurements of change. Quantification errors, or inconsistencies between

timepoints, is one of the biggest sources of uncertainty, and this could be addressed through longitudinal registration pipelines. Finally, the low temporal precision of the ARC relative to the small magnitude of change detectable means that studies should include always include an estimation the ARC variability.

Intrinsic variability both within and between subjects results from biological factors, that, if controlled or accounted for, could reduce the overall variation in the rate of change in amyloid or tau. On top of age, genetic profile, and comorbid conditions, female sex and race/ethnicity could contribute to longitudinal variability and impact the rate of AD-protein accumulation. In addition, disease subtype and staging models could help characterize the spatiotemporal disease heterogeneity in these modalities, thereby allowing for more precise estimates of disease progression that could be reflected by distinct Aβ or tau accumulation patterns. At the individual level, PET variability is driven mainly by blood flow and atrophy, which could be addressed, in some cases, by dynamic acquisitions and an appropriate PVC technique (two-compartment or three-compartment PVC for ^{11}C-PiB).

The studies selected and reviewed depict the state of the art of the literature focused on longitudinal amyloid and tau PET. One limitation, however, is that numerous studies use longitudinal PET without ARC as one of the main dependent outcomes analyzed. We also acknowledge that the level of details in reporting methodologies is guided by the focus of the paper and limited by journal editorial constraints, and that more comprehensive information could be available upon request. Finally, translating technological progress into methodological advances achievable in a research and clinical setting can be difficult. As a result, addressing the sources of variability summarized here is not always feasible because of time, cost, skills required, or software availability constraints.

Several questions about how and when to best address those sources of variability remain to be explored. First regarding biological factors, although the impact of atrophy and blood flow fluctuations can be mitigated using PVC and dynamic imaging, both of those solutions can introduce additional noise. Their appropriate use in a longitudinal setting is dependent on the advancement of AD at the individual level, and on the true amyloid accumulation within the time window in-between PET scans. For instance, for subjects in the later stages of the disease more likely to have pronounced atrophy, PVC is necessary to avoid underestimating the AD-protein accumulation. Defining the level of atrophy above which PVC should be applied, taking into account the duration of the study, investigating the best PVC method to use longitudinally for all available tracers, or presenting results both with and without atrophy could help address some of the debates around PVC usage. How to balance precision and accuracy should also be explored to evaluate the acquisition of longitudinal static versus dynamic acquisitions. Indeed, although the latter is less susceptible to variations in blood flow, the BP_{ND} or DVR derived from these acquisitions might be noisier, have a narrower dynamic range and are less feasible, in terms of time and cost, for many clinical research scenarios than SUVr and CL outcomes based on static acquisition.

Another factor that could play a role in AD-protein accumulation is resilience in the form of cognitive reserve and brain maintenance. Investigating how those mechanisms influence AD-protein accumulation could possibly enhance disease-prediction models.

Despite the numerous questions around how to control or mitigate biological and physiological variability, there are many areas where technical factors could be improved further and reduce measurement error. Although the impact of motion on quantification has been investigated, and many motion correction approaches exist, it has yet to be consistently implemented in processing pipelines and reported in the methodology of articles. For motion correction, guidelines defining acceptable levels of motion based on whether the gain in accuracy and the gain in signal is greater than the uncertainty introduced by the registration and resampling/interpolation processes could be developed. As motion is not always easily detectable and data sets continue to grow in size, systematic motion detection and quantification techniques will be particularly important to ensure that automated pipelines produce accurate AD-protein quantification.

Further research could focus the characterization of the ARC (1) at the individual level and (2) across the AD continuum, considering the non-linearity of amyloid and tau accumulation over time. In addition, consistent strategies to define accumulators versus stable trajectories could increase comparability of different studies. On the other hand, a varying percentage of negative ARC is also observed, especially in individuals with low amyloid burden. Better understanding of the potential technical factors leading to those results could help either improve the performance of the ARC metric or better define the amyloid hypothesis in the earliest stages of the disease.

The next crucial step to improve the interpretability and reproducibility of longitudinal studies is to generalize the use of standardization and harmonization strategies.

Multinational and international standards developed for the use of amyloid PET by the Society of Nuclear Medicine and Molecular Imaging and the European Association of Nuclear Medicine[190] and by the Radiological Society of North America QIBA[101] should be followed. Regarding tau, an international consensus for the use of ^{18}F-flortaucipir was also published.[191]

Starting with the acquisition of the scans, several aspects of the processing can be harmonized such as the effective spatial resolution of PET images obtained from different reconstruction protocols[192,193] and the data acquired in multiple centers.[194,195] Standardization of the processing and analysis can then be considered, including standardization of the PET outcome metrics across amyloid,[150,169,196,197] and tau tracers or using open-source processing pipelines such as the PET Unified Pipeline PUP,[198] the robust PET-only processing rPOP,[199] or the Computational analysis of PET by AIBL CapAIBL.[200] Establishing standards of reporting ARC measures would also increase the comparability and reproducibility across studies.

In the absence of ground-truth, the evaluation of comprehensive reproducible pipelines is challenging. However, several strategies can be implemented to determine how to generate the most precise and clinically valuable ARC estimates (see more details in Supplementary Material). Overall, there is a need for unified frameworks specifically designed for longitudinal quantitative PET studies.

8 | CONCLUSION

Measuring longitudinal change in amyloid and tau deposition via PET provides valuable insights into the pathophysiology of AD; however, distinguishing noise from actual protein accumulation is challenging. In this review, we proposed a comprehensive review of the major factors that can impact longitudinal PET quantification, supported by a systematic search of the literature. With the increased number of longitudinal PET studies, some of the factors of variability first posed by Schmidt et al. have now been tested and their impact on measurement precision has been quantified. Finally, we highlighted longitudinal-PET specific processing pipelines and how they could leverage the shared information between same-subject scans, help control intrinsic variability, and reduce measurement uncertainty.

ACKNOWLEDGMENTS

This work is supported by the EPSRC-funded UCL Centre for Doctoral Training in Intelligent, Integrated Imaging in Healthcare (i4health) (EP/S021930/1), the Department of Health's NIHR-funded Biomedical Research Centre at University College London, and GE Healthcare. The project leading to this paper has also received funding from the Innovative Medicines Initiative 2 Joint Undertaking under grant agreement No 115952. This Joint Undertaking receives the support from the European Union's Horizon 2020 research and innovation programme and EFPIA. This communication reflects the views of the authors and neither IMI nor the European Union and EFPIA are liable for any use that may be made of the information contained herein.

CONFLICT OF INTEREST STATEMENT

Ariane Bollack, Pawel Markiewicz, and David M. Cash report no relevant disclosures. Hugh G Pemberton is a former GE HealthCare employee. Lyduine E. Collij has received research support from GE HealthCare (paid to institution). Gill Farrar is an employee of GE Healthcare. Frederik Barkhof is a steering committee and iDMC member of studies by Biogen, Merck, Roche, EISAI, and Prothena. He is a consultant to Roche, Biogen, Merck, IXICO, Jansen, and Combinostics. He has research agreements with Merck, Biogen, GE Healthcare, and Roche and is co-founder and shareholder of Queen Square Analytics Ltd. Author disclosures are available in the Supporting Information.

ORCID

Ariane Bollack https://orcid.org/0000-0002-9169-7530
Hugh G. Pemberton https://orcid.org/0000-0001-8419-6423
Lyduine E. Collij https://orcid.org/0000-0001-6263-1762
Pawel Markiewicz https://orcid.org/0000-0002-3114-0773
David M. Cash https://orcid.org/0000-0001-7833-616X
Frederik Barkhof https://orcid.org/0000-0003-3543-3706

REFERENCES

1. Jack CR, Knopman DS, Jagust WJ, et al. Tracking pathophysiological processes in Alzheimer's disease: an updated hypothetical model of dynamic biomarkers. *Lancet Neurol*. 2013;12(2):207-216. doi: 10.1016/S1474-4422(12)70291-0
2. Villemagne VL, Burnham S, Bourgeat P, et al. Amyloid β deposition, neurodegeneration, and cognitive decline in sporadic Alzheimer's disease: a prospective cohort study. *Lancet Neurol*. 2013;12(4):357-367. doi: 10.1016/S1474-4422(13)70044-9
3. Gordon BA, Blazey TM, Su Y, et al. Spatial patterns of neuroimaging biomarker change in individuals from families with autosomal dominant Alzheimer's disease: a longitudinal study. *Lancet Neurol*. 2018;17(3):241-250.
4. Villemagne VL, Pike KE, Chételat G, et al. Longitudinal assessment of Aβ and cognition in aging and Alzheimer disease. *Ann Neurol*. 2011;69(1):181-192. doi: 10.1002/ana.22248
5. Jack CR, Wiste HJ, Schwarz CG, et al. Longitudinal tau PET in ageing and Alzheimer's disease. *Brain*. 2018;141(5):1517-1528.
6. Harn NR, Hunt SL, Hill J, Vidoni E, Perry M, Burns JM. Augmenting amyloid PET interpretations with quantitative information improves consistency of early amyloid detection. *Clin Nucl Med*. 2017;42(8):577-581. doi: 10.1097/RLU.0000000000001693
7. Pemberton HG, Collij LE, Heeman F, et al. Quantification of amyloid PET for future clinical use: a state-of-the-art review. *Eur J Nucl Med Mol Imaging*. 2022;49(10):3508-3528. doi: 10.1007/s00259-022-05784-y Published online April 7, 2022
8. Verdi S, Marquand AF, Schott JM, Cole JH. Beyond the average patient: how neuroimaging models can address heterogeneity in dementia. *Brain*. 2021;144(10):2946-2953. Published online 2021.
9. Budd Haeberlein S, Aisen PS, Barkhof F, et al. Two randomized phase 3 studies of aducanumab in early Alzheimer's disease. *J Prev Alzheimers Dis*. 2022;9(2):197-210. 10.14283/jpad.2022.30 Published online 2022
10. Mintun MA, Lo AC, Duggan Evans C, et al. Donanemab in early Alzheimer's disease. *N Engl J Med*. 2021;384(18):1691-1704. doi: 10.1056/NEJMoa2100708
11. Swanson CJ, Zhang Y, Dhadda S, et al. A randomized, double-blind, phase 2b proof-of-concept clinical trial in early Alzheimer's disease with lecanemab, an anti-Aβ protofibril antibody. *Alzheimers Res Ther*. 2021;13(1):80. doi: 10.1186/s13195-021-00813-8
12. Salloway S, Farlow M, McDade E, et al. A trial of gantenerumab or solanezumab in dominantly inherited Alzheimer's disease. *Nat Med*. 2021;27(7):1187-1196. doi: 10.1038/s41591-021-01369-8
13. Schmidt ME, Chiao P, Klein G, et al. The influence of biological and technical factors on quantitative analysis of amyloid PET: points to consider and recommendations for controlling variability in longitudinal data. *Alzheimers Dement*. 2015;11(9):1050-1068. doi: 10.1016/j.jalz.2014.09.004
14. Cash DM, Frost C, Iheme LO, et al. Assessing atrophy measurement techniques in dementia: results from the MIRIAD atrophy challenge. *NeuroImage*. 2015;123:149-164. doi: 10.1016/j.neuroimage.2015.07.087
15. Gordon BA, McCullough A, Mishra S, et al. Cross-sectional and longitudinal atrophy is preferentially associated with tau rather than amyloid β positron emission tomography pathology. *Alzheimers Dement Diagn Assess Dis Monit*. 2018;10:245-252. doi: 10.1016/j.dadm.2018.02.003
16. Reuter M, Schmansky NJ, Rosas HD, Fischl B. Within-subject template estimation for unbiased longitudinal image analysis. *NeuroImage*. 2012;61(4):1402-1418. doi: 10.1016/j.neuroimage.2012.02.084
17. Holland D, Dale AM. Nonlinear registration of longitudinal images and measurement of change in regions of interest. *Med Image Anal*. 2011;15(4):489-497. doi: 10.1016/j.media.2011.02.005
18. Moher D, Liberati A, Tetzlaff L, Altman DG, PRISMA Group. Preferred reporting items for systematic reviews and meta-analyses: the PRISMA statement. *PLoS Med*. 2009;6(7):e1000097. doi: 10.1371/journal.pmed.1000097
19. Knudsen GM, Ganz M, Appelhoff S, et al. Guidelines for the content and format of PET brain data in publications and archives: a

consensus paper. *J Cereb Blood Flow Metab*. 2020;40(8):1576-1585. doi: 10.1177/0271678x20905433
20. Rousset OG. Correction for partial volume effects in PET: principle and validation. *J Nucl Med*. 1998;39(5):904-911.
21. Meltzer CC, Leal JP, Mayberg HS, Wagner HN, Frost JJ. Correction of PET data for partial volume effects in human cerebral cortex by MR imaging. *J Comput Assist Tomogr*. 1990;14(4):561-570. doi: 10.1097/00004728-199007000-00011
22. Müller-Gärtner HW, Links JM, Prince JL, et al. Measurement of radiotracer concentration in brain gray matter using positron emission tomography: MRI-based correction for partial volume effects. *J Cereb Blood Flow Metab*. 1992;12(4):571-583. doi: 10.1038/jcbfm.1992.81
23. Klein G, Delmar P, Voyle N, et al. Gantenerumab reduces amyloid-β plaques in patients with prodromal to moderate Alzheimer's disease: a PET substudy interim analysis. *Alzheimers Res Ther*. 2019;11(1):101. doi: 10.1186/s13195-019-0559-z
24. Lowe SL, Duggan Evans C, Shcherbinin S, et al. Donanemab (LY3002813) Phase 1b Study in Alzheimer's disease: rapid and sustained reduction of brain amyloid measured by Florbetapir F18 imaging. *J Prev Alzheimers Dis*. 2021;8(4):414-424. 10.14283/jpad.2021.56
25. Leal SL, Lockhart SN, Maass A, Bell RK, Jagust WJ. Subthreshold amyloid predicts Tau deposition in aging. *J Neurosci*. 2018;38(19):4482-4489. doi: 10.1523/JNEUROSCI.0485-18.2018
26. Hanseeuw BJ, Betensky RA, Jacobs HIL, et al. Association of amyloid and Tau with cognition in preclinical Alzheimer disease: a longitudinal study. *JAMA Neurol*. 2019;76(8):915-924. doi: 10.1001/jamaneurol.2019.1424
27. Kim YJ, Seo SW, Park SB, et al. Protective effects of APOE e2 against disease progression in subcortical vascular mild cognitive impairment patients: a three-year longitudinal study. *Sci Rep*. 2017;7(1):1910. doi: 10.1038/s41598-017-02046-y
28. Lao PJ, Brickman AM, Alzheimer's Disease Neuroimaging Initiative. Multimodal neuroimaging study of cerebrovascular disease, amyloid deposition, and neurodegeneration in Alzheimer's disease progression. *Alzheimers Dement Diagn Assess Dis Monit*. 2018;10(1):638-646. doi: 10.1016/j.dadm.2018.08.007
29. Leal SL, Landau SM, Bell RK, Jagust WJ. Hippocampal activation is associated with longitudinal amyloid accumulation and cognitive decline. *eLife*. 2017;6:e22978. doi: 10.7554/eLife.22978
30. Lim YY, Mormino EC, Alzheimer's Disease Neuroimaging Initiative. APOE genotype and early β-amyloid accumulation in older adults without dementia. *Neurology*. 2017;89(10):1028-1034. doi: 10.1212/WNL.0000000000004336
31. Lopes Alves I, Heeman F, Collij LE, et al. Strategies to reduce sample sizes in Alzheimer's disease primary and secondary prevention trials using longitudinal amyloid PET imaging. *Alzheimers Res Ther*. 2021;13(1):82. doi: 10.1186/s13195-021-00819-2
32. Lopresti BJ, Campbell EM, Yu Z, et al. Influence of apolipoprotein-E genotype on brain amyloid load and longitudinal trajectories. *Neurobiol Aging*. 2020;94:111-120. doi: 10.1016/j.neurobiolaging.2020.05.012
33. Lowe VJ, Lundt ES, Senjem ML, et al. White matter reference region in PET studies of ^{11} C-Pittsburgh Compound B uptake: effects of age and Amyloid-β deposition. *J Nucl Med*. 2018;59(10):1583-1589. doi: 10.2967/jnumed.117.204271
34. Mishra S, Blazey TM, Holtzman DM, et al. Longitudinal brain imaging in preclinical Alzheimer disease: impact of APOE ε4 genotype. *Brain*. 2018;141(6):1828-1839. doi: 10.1093/brain/awy103
35. Resnick SM, Bilgel M, Moghekar A, et al. Changes in Aβ biomarkers and associations with APOE genotype in 2 longitudinal cohorts. *Neurobiol Aging*. 2015;36(8):2333-2339. doi: 10.1016/j.neurobiolaging.2015.04.001
36. Rodriguez-Vieitez E, Saint-Aubert L, Carter SF, et al. Diverging longitudinal changes in astrocytosis and amyloid PET in autosomal dominant Alzheimer's disease. *Brain*. 2016;139(3):922-936. doi: 10.1093/brain/awv404
37. Su Y, Hornbeck RC, Speidel B, et al. Comparison of Pittsburgh compound B and florbetapir in cross-sectional and longitudinal studies. *Alzheimers Dement Diagn Assess Dis Monit*. 2019;11(1):180-190. doi: 10.1016/j.dadm.2018.12.008
38. Shokouhi S, Riddle W, Kang H. A new data analysis approach for measuring longitudinal changes of metabolism in cognitively normal elderly adults. *Clin Interv Aging*. 2017;12:2123-2130. doi: 10.2147/CIA.S150859
39. Pereira JB, Harrison TM, La Joie R, Baker SL, Jagust WJ. Spatial patterns of tau deposition are associated with amyloid, ApoE, sex, and cognitive decline in older adults. *Eur J Nucl Med Mol Imaging*. 2020;47(9):2155-2164. doi: 10.1007/s00259-019-04669-x
40. Lee J, Burkett BJ, Min HK, et al. The overlap index as a means of evaluating early tau-PET signal reliability. *J Nucl Med*;63(11):1748-1753. doi: 10.2967/jnumed.121.263136 Published online March 17, 2022:jnumed.121.263136
41. Mi L, Zhang W, Zhang J, et al. An optimal transportation based univariate neuroimaging index. *Proc IEEE Int Conf Comput Vis*. 2017;2017:182-191.
42. Vandenberghe R, Van Laere K, Ivanoiu A, et al. 18F-flutemetamol amyloid imaging in Alzheimer disease and mild cognitive impairment: a phase 2 trial: 18F-Flutemetamol Phase 2 Trial. *Ann Neurol*. 2010;68(3):319-329. doi: 10.1002/ana.22068
43. Lopresti BJ, Klunk WE, Mathis CA, et al. Simplified quantification of Pittsburgh compound B amyloid imaging PET studies: a comparative analysis. *J Nucl Med*. 2005;46(12):1959-1972. Published online 2005.
44. Tolboom N, Yaqub M, Boellaard R, et al. Test-retest variability of quantitative [11C]PIB studies in Alzheimer's disease. *Eur J Nucl Med Mol Imaging*. 2009;36(10):1629-1638. doi: 10.1007/s00259-009-1129-6
45. Sabri O, Sabbagh MN, Seibyl J, et al. Florbetaben PET imaging to detect amyloid beta plaques in Alzheimer's disease: phase 3 study. *Alzheimers Dement*. 2015;11(8):964-974. doi: 10.1016/j.jalz.2015.02.004
46. Neuraceq - Public Assessment Report. Published online 2014. Accessed January 17, 2022. https://www.ema.europa.eu/en/documents/assessment-report/neuraceq-epar-public-assessment-report_en.pdf
47. Barthel H, Bullich S, Sabri O, et al. 18F-Florbetaben (FBB) PET SUVR quantification: which reference region? *J Nucl Med*. 2015;56(3):1563-1563.
48. Landau SM, Fero A, Baker SL, et al. Measurement of longitudinal -amyloid change with 18F-Florbetapir PET and standardized uptake value ratios. *J Nucl Med*. 2015;56(4):567-574. doi: 10.2967/jnumed.114.148981
49. Joshi AD, Pontecorvo MJ, Clark CM, et al. Performance characteristics of amyloid PET with Florbetapir F 18 in patients with Alzheimer's disease and cognitively normal subjects. *J Nucl Med*. 2012;53(3):378-384. doi: 10.2967/jnumed.111.090340
50. Verfaillie SC, Golla SS, Timmers T, et al. Repeatability of parametric methods for [18 F]florbetapir imaging in Alzheimer's disease and healthy controls: a test–retest study. *J Cereb Blood Flow Metab*. 2021;41(3):569-578. doi: 10.1177/0271678x20915403
51. Devous MD, Joshi AD, Navitsky M, et al. Test–Retest reproducibility for the Tau PET imaging agent Flortaucipir F 18. *J Nucl Med*. 2018;59(6):937-943. doi: 10.2967/jnumed.117.200691
52. Whittington A, Gunn R. Tau^{IQ} - a canonical image based algorithm to quantify tau PET scans. *J Nucl Med*. 2021;62(9):1292-1300. doi: 10.2967/jnumed.120.258962 Published online January 30, 2021:jnumed.120.258962
53. Pontecorvo MJ, Devous MD, Kennedy I, et al. A multicentre longitudinal study of flortaucipir (18F) in normal ageing, mild cognitive

impairment and Alzheimer's disease dementia. *Brain*. 2019;142(6):1723-1735. doi: 10.1093/brain/awz090

54. Harrison TM, La Joie R, Maass A, et al. Longitudinal tau accumulation and atrophy in aging and Alzheimer disease: tau-PET and Atrophy. *Ann Neurol*. 2019;85(2):229-240. doi: 10.1002/ana.25406
55. van Belle G. *Statistical rules of thumb*. John Wiley & Sons; 2011.
56. Riedel BC, Thompson PM, Brinton RD. Age, APOE and sex: triad of risk of Alzheimer's disease. *J Steroid Biochem Mol Biol*. 2016;160:134-147. doi: 10.1016/j.jsbmb.2016.03.012
57. Evans DA, Bennett DA, Wilson RS, et al. Incidence of Alzheimer disease in a biracial urban community: relation to apolipoprotein E allele status. *Arch Neurol*. 2003;60(2):185. doi: 10.1001/archneur.60.2.185
58. Tang MX. The APOE-ϵ4 allele and the risk of Alzheimer disease among African Americans, Whites, and Hispanics. *JAMA*. 1998;279(10):751. doi: 10.1001/jama.279.10.751
59. Burnham SC, Laws SM, Budgeon CA, et al. Impact of APOE-ε4 carriage on the onset and rates of neocortical Aβ-amyloid deposition. *Neurobiol Aging*. 2020;95:46-55. doi: 10.1016/j.neurobiolaging.2020.06.001
60. Jansen WJ, Ossenkoppele R, Knol DL, et al. Prevalence of cerebral amyloid pathology in persons without dementia: a meta-analysis. *JAMA*. 2015;313(19):1924-1938. doi: 10.1001/jama.2015.4668
61. Betthauser TJ, Bilgel M, Koscik RL, et al. Multi-method investigation of factors influencing amyloid onset and impairment in three cohorts. *Brain*. 2022;145(11):4065-4079. Published online 2022.
62. Grimmer T, Tholen S, Yousefi BH, et al. Progression of cerebral amyloid load is associated with the Apolipoprotein E ε4 Genotype in Alzheimer's disease. *Biol Psychiatry*. 2010;68(10):879-884. doi: 10.1016/j.biopsych.2010.05.013
63. Baek MS, Cho H, Lee HS, Lee JH, Ryu YH, Lyoo CH. Effect of APOE ε4 genotype on amyloid-β and tau accumulation in Alzheimer's disease. *Alzheimers Res Ther*. 2020;12(1):140. doi: 10.1186/s13195-020-00710-6
64. Mazure CM, Swendsen J. Sex differences in Alzheimer's disease and other dementias. *Lancet Neurol*. 2016;15(5):451-452. doi: 10.1016/S1474-4422(16)00067-3
65. Buckley RF, Mormino EC, Rabin JS, et al. Sex differences in the association of global amyloid and regional Tau deposition measured by positron emission tomography in clinically normal older adults. *JAMA Neurol*. 2019;76(5):542. doi: 10.1001/jamaneurol.2018.4693
66. Smith R, Strandberg O, Mattsson-Carlgren N, et al. The accumulation rate of tau aggregates is higher in females and younger amyloid-positive subjects. *Brain*. 2020;143(12):3805-3815. doi: 10.1093/brain/awaa327
67. Morris JC, Schindler SE, McCue LM, et al. Assessment of racial disparities in biomarkers for Alzheimer disease. *JAMA Neurol*. 2019;76(3):264-273. doi: 10.1001/jamaneurol.2018.4249
68. Deters KD, Napolioni V, Sperling RA, et al. Amyloid PET imaging in self-identified Non-Hispanic black participants of the anti-amyloid in asymptomatic Alzheimer's disease (A4) study. *Neurology*. 2021;96(11):e1491-e1500. doi: 10.1212/WNL.0000000000011599
69. Wilkins CH, Windon CC, Dilworth-Anderson P, et al. Racial and Ethnic differences in amyloid PET positivity in individuals with mild cognitive impairment or dementia: a secondary analysis of the Imaging Dementia–Evidence for Amyloid Scanning (IDEAS) Cohort Study. *JAMA Neurol*. 2022;79(11):1139-1147. doi: 10.1001/jamaneurol.2022.3157 Published online October 3, 2022
70. Jin M, Kennedy G, Deters KD, et al. Reduced amyloid and greater neuropsychological testing exclusion in the A4 study in individuals that self-identify as non-Hispanic Asian. *Alzheimers Dement*. 2021;17(S10):e055614. doi: 10.1002/alz.055614
71. Meeker KL, Wisch JK, Hudson D, et al. Socioeconomic status mediates racial differences seen using the AT(N) framework. *Ann Neurol*. 2021;89(2):254-265. doi: 10.1002/ana.25948
72. Lee CM, Jacobs HIL, Marquié M, et al. 18F-Flortaucipir Binding in choroid plexus: related to race and hippocampus signal. *J Alzheimers Dis*. 2018;62(4):1691-1702. doi: 10.3233/JAD-170840
73. Ziontz J, Bilgel M, Shafer AT, et al. Tau pathology in cognitively normal older adults. *Alzheimers Dement Diagn Assess Dis Monit*. 2019;11:637-645. doi: 10.1016/j.dadm.2019.07.007
74. van Nieuwpoort F, Smit NPM, Kolb R, van der Meulen H, Koerten H, Pavel S. Tyrosine-induced melanogenesis shows differences in morphologic and melanogenic preferences of melanosomes from light and dark skin types. *J Invest Dermatol*. 2004;122(5):1251-1255. doi: 10.1111/j.0022-202X.2004.22533.x
75. Canevelli M, Bruno G, Grande G, et al. Race reporting and disparities in clinical trials on Alzheimer's disease: a systematic review. *Neurosci Biobehav Rev*. 2019;101:122-128. doi: 10.1016/j.neubiorev.2019.03.020
76. Barnes LL. Alzheimer disease in African American individuals: increased incidence or not enough data? *Nat Rev Neurol*. 2022;18(1):56-62. doi: 10.1038/s41582-021-00589-3
77. Sintini I, Martin PR, Graff-Radford J, et al. Longitudinal tau-PET uptake and atrophy in atypical Alzheimer's disease. *NeuroImage Clin*. 2019;23:101823. doi: 10.1016/j.nicl.2019.101823
78. Phillips JS, Nitchie FJ, Da Re F, et al. Rates of longitudinal change in ^{18}F-flortaucipir PET vary by brain region, cognitive impairment, and age in atypical Alzheimer's disease. *Alzheimers Dement*. 2022;18(6):1235-1247. doi: 10.1002/alz.12456
79. Sintini I, Graff-Radford J, Senjem ML, et al. Longitudinal neuroimaging biomarkers differ across Alzheimer's disease phenotypes. *Brain*. 2020;143(7):2281-2294. doi: 10.1093/brain/awaa155
80. Grothe MJ, Barthel H, Sepulcre J, et al. In vivo staging of regional amyloid deposition. *Neurology*. 2017;89(20):2031-2038. doi: 10.1212/WNL.0000000000004643
81. Hanseeuw BJ, Betensky RA, Mormino EC, et al. PET staging of amyloidosis using striatum. *Alzheimers Dement*. 2018;14(10):1281-1292. doi: 10.1016/j.jalz.2018.04.011
82. Mattsson N, Palmqvist S, Stomrud E, Vogel J, Hansson O. Staging β-Amyloid pathology with amyloid positron emission tomography. *JAMA Neurol*. 2019;76(11):1319-1329. doi: 10.1001/jamaneurol.2019.2214
83. Jelistratova I, Teipel SJ, Grothe MJ. Longitudinal validity of PET-based staging of regional amyloid deposition. *Hum Brain Mapp*. 2020;41(15):4219-4231. doi: 10.1002/hbm.25121
84. Chen SD, Lu JY, Li HQ, et al. Staging tau pathology with tau PET in Alzheimer's disease: a longitudinal study. *Transl Psychiatry*. 2021;11(1):1-12. doi: 10.1038/s41398-021-01602-5
85. Yang F, Chowdhury SR, Jacobs HIL, et al. Longitudinal predictive modeling of tau progression along the structural connectome. *NeuroImage*. 2021;237:118126. doi: 10.1016/j.neuroimage.2021.118126
86. Vogel JW, Young AL, Oxtoby NP, et al. Four distinct trajectories of tau deposition identified in Alzheimer's disease. *Nat Med*. 2021;27(5):871-881. doi: 10.1038/s41591-021-01309-6
87. Hillmer AT, Carson RE. Quantification of PET infusion studies without true equilibrium: a tissue clearance correction. *J Cereb Blood Flow Metab*. 2020;40(4):860-874. doi: 10.1177/0271678x19850000
88. Zhou Y, Flores S, Mansor S, et al. Spatially constrained kinetic modeling with dual reference tissues improves 18F-flortaucipir PET in studies of Alzheimer disease. *Eur J Nucl Med Mol Imaging*. 2021;48(10):3172-3186. doi: 10.1007/s00259-020-05134-w Published online February 18, 2021
89. Bullich S, Barthel H, Koglin N, et al. Effect of cerebral blood flow changes on 18F-florbetaben SUVR. *J Nucl Med*. 2019;60(1):1180-1180.
90. van Berckel BNM, Ossenkoppele R, Tolboom N, et al. Longitudinal amyloid imaging using ^{11} C-PiB: methodologic considerations. *J Nucl Med*. 2013;54(9):1570-1576. doi: 10.2967/jnumed.112.113654

91. Bilgel M, Beason-Held L, An Y, Zhou Y, Wong DF, Resnick SM. Longitudinal evaluation of surrogates of regional cerebral blood flow computed from dynamic amyloid PET imaging. *J Cereb Blood Flow Metab*. 2020;40(2):288-297. doi: 10.1177/0271678x19830537
92. Clement P, Mutsaerts HJ, Václavů L, et al. Variability of physiological brain perfusion in healthy subjects – A systematic review of modifiers. Considerations for multi-center ASL studies. *J Cereb Blood Flow Metab*. 2018;38(9):1418-1437. doi: 10.1177/0271678x17702156
93. Ottoy J, Verhaeghe J, Niemantsverdriet E, Engelborghs S, Stroobants S, Staelens S. A simulation study on the impact of the blood flow-dependent component in [18F]AV45 SUVR in Alzheimer's disease. *PLOS ONE*. 2017;12(12):e0189155. doi: 10.1371/journal.pone.0189155
94. Cselényi Z, Farde L. Quantification of blood flow-dependent component in estimates of beta-amyloid load obtained using quasi-steady-state standardized uptake value ratio. *J Cereb Blood Flow Metab*. 2015;35(9):1485-1493. doi: 10.1038/jcbfm.2015.66
95. Heeman F, Yaqub M, Lopes Alves I, et al. Simulating the effect of cerebral blood flow changes on regional quantification of [18F]flutemetamol and [18F]florbetaben studies. *J Cereb Blood Flow Metab*. 2021;41(3):579-589. doi: 10.1177/0271678x20918029 Published online April 11, 2020:0271678x20918029
96. Chen YJ, Rosario BL, Mowrey W, et al. Relative 11C-PiB delivery as a proxy of relative CBF: quantitative evaluation using single-session 15O-Water and 11C-PiB PET. *J Nucl Med*. 2015;56(8):1199-1205. doi: 10.2967/jnumed.114.152405
97. Heeman F, Hendriks J, Lopes Alves I, et al. Test-retest variability of relative tracer delivery rate as measured by [11C]PiB. *Mol Imaging Biol*. 2021;23(3):335-339. doi: 10.1007/s11307-021-01606-z
98. Heeman F, Yaqub M, Hendriks J, et al. Impact of cerebral blood flow and amyloid load on SUVR bias. *EJNMMI Res*. 2022;12(1):29. doi: 10.1186/s13550-022-00898-8
99. Lockhart SN, Baker SL, Okamura N. Dynamic PET measures of tau accumulation in cognitively normal older adults and Alzheimer's disease patients measured using [18F] THK-5351. *PLOS ONE*. 2016;11(6):e0158460. doi: 10.1371/journal.pone.0158460
100. Chen KT, Salcedo S, Chonde DB, et al. MR-assisted PET motion correction in simultaneous PET/MRI studies of dementia subjects: mR-Assisted PET Motion correction. *J Magn Reson Imaging*. 2018;48(5):1288-1296. doi: 10.1002/jmri.26000
101. Smith AM, Obuchowski NA, Foster NL, et al. The RSNA QIBA profile for amyloid PET as an imaging biomarker for cerebral amyloid quantification. *J Nucl Med*. 2023;64(2):294-303. doi: 10.2967/jnumed.122.264031
102. Reader AJ, Corda G, Mehranian A, da Costa-Luis C, Ellis S, Schnabel JA. Deep learning for PET image reconstruction. *IEEE Trans Radiat Plasma Med Sci*. 2021;5(1):1-25. doi: 10.1109/TRPMS.2020.3014786
103. Gong K, Catana C, Qi J, Li Q. PET image reconstruction using deep image prior. *IEEE Trans Med Imaging*. 2019;38(7):1655-1665. doi: 10.1109/TMI.2018.2888491
104. Spangler-Bickell MG, Deller TW, Bettinardi V, Jansen F. Ultra-fast list-mode reconstruction of short PET frames and example applications. *J Nucl Med Off Publ Soc Nucl Med*. 2021;62(2):287-292. doi: 10.2967/jnumed.120.245597
105. Gillman A, Smith J, Thomas P, Rose S, Dowson N. PET motion correction in context of integrated PET/MR: current techniques, limitations, and future projections. *Med Phys*. 2017;44(12):e430-e445. doi: 10.1002/mp.12577
106. Markiewicz PJ, Matthews JC, Ashburner J, et al. Uncertainty analysis of MR-PET image registration for precision neuro-PET imaging. *NeuroImage*. 2021;232:117821. doi: 10.1016/j.neuroimage.2021.117821
107. Schwarz CG, Jones DT, Gunter JL, et al. Contributions of imprecision in PET-MRI rigid registration to imprecision in amyloid PET SUVR measurements. *Hum Brain Mapp*. 2017;38(7):3323-3336. doi: 10.1002/hbm.23622
108. Knudsen GM, Ganz M, Appelhoff S, et al. Guidelines for the content and format of PET brain data in publications and archives: a consensus paper. *J Cereb Blood Flow Metab*. 2020;40(8):1576-1585. doi: 10.1177/0271678x20905433 Published online February 16, 2020:0271678x20905433
109. Heeman F, Yaqub M, Lopes Alves I, et al. Optimized dual-time-window protocols for quantitative [18F]flutemetamol and [18F]florbetaben PET studies. *EJNMMI Res*. 2019;9(1):32. doi: 10.1186/s13550-019-0499-4
110. Tuncel H, Visser D, Yaqub M, et al. Effect of shortening the scan duration on quantitative accuracy of [18F]Flortaucipir studies. *Mol Imaging Biol*. 2021;23(4):604-613. doi: 10.1007/s11307-021-01581-5
111. Shcherbinin S, Schwarz AJ, Joshi A, et al. Kinetics of the Tau PET Tracer ^{18} F-AV-1451 (T807) in subjects with normal cognitive function, mild cognitive impairment, and Alzheimer disease. *J Nucl Med*. 2016;57(10):1535-1542. doi: 10.2967/jnumed.115.170027
112. Barret O, Alagille D, Sanabria S, et al. Kinetic Modeling of the Tau PET Tracer 18F-AV-1451 in human healthy volunteers and Alzheimer disease subjects. *J Nucl Med*. 2017;58(7):1124-1131. doi: 10.2967/jnumed.116.182881
113. Kolinger GD, Vállez García D, Lohith TG, et al. A dual-time-window protocol to reduce acquisition time of dynamic tau PET imaging using [18F]MK-6240. *EJNMMI Res*. 2021;11(1):49. doi: 10.1186/s13550-021-00790-x
114. Slart RHJA, Tsoumpas C, Glaudemans AWJM, et al. Long axial field of view PET scanners: a road map to implementation and new possibilities. *Eur J Nucl Med Mol Imaging*. 2021;48(13):4236-4245. doi: 10.1007/s00259-021-05461-6
115. Badawi RD, Shi H, Hu P, et al. First human imaging studies with the EXPLORER Total-Body PET Scanner*. *J Nucl Med*. 2019;60(3):299-303. doi: 10.2967/jnumed.119.226498
116. Alberts I, Hünermund JN, Prenosil G, et al. Clinical performance of long axial field of view PET/CT: a head-to-head intra-individual comparison of the Biograph Vision Quadra with the Biograph Vision PET/CT. *Eur J Nucl Med Mol Imaging*. 2021;48(8):2395-2404. doi: 10.1007/s00259-021-05282-7
117. Cherry SR, Jones T, Karp JS, Qi J, Moses WW, Badawi RD. Total-body PET: maximizing sensitivity to create new opportunities for clinical research and patient care. *J Nucl Med*. 2018;59(1):3-12. doi: 10.2967/jnumed.116.184028
118. Abgral R, Bourhis D, Salaun PY. Clinical perspectives for the use of total body PET/CT. *Eur J Nucl Med Mol Imaging*. 2021;48(6):1712-1718. doi: 10.1007/s00259-021-05293-4
119. Kang J, Gao Y, Shi F, Lalush DS, Lin W, Shen D. Prediction of standard-dose brain PET image by using MRI and low-dose brain [18F]FDG PET images. *Med Phys*. 2015;42(9):5301-5309. doi: 10.1118/1.4928400
120. Xiang L, Qiao Y, Nie D, et al. Deep auto-context convolutional neural networks for standard-dose PET image estimation from low-dose PET/MRI. *Neurocomputing*. 2017;267:406-416. doi: 10.1016/j.neucom.2017.06.048
121. Nai YH, Watanuki S, Tashiro M, Okamura N, Watabe H. Investigation of the quantitative accuracy of low-dose amyloid and tau PET imaging. *Radiol Phys Technol*. 2018;11(4):451-459. doi: 10.1007/s12194-018-0485-y
122. Chen KT, Gong E, de Carvalho Macruz FB, et al. Ultra–low-dose 18F-Florbetaben amyloid PET imaging using deep learning with multi-contrast MRI inputs. *Radiology*. 2019;290(3):649-656. doi: 10.1148/radiol.2018180940
123. Thomas BA, Erlandsson K, Modat M, et al. The importance of appropriate partial volume correction for PET quantification in Alzheimer's disease. *Eur J Nucl Med Mol Imaging*. 2011;38(6):1104-1119. doi: 10.1007/s00259-011-1745-9

124. Blautzik J, Brendel M, Sauerbeck J, et al. Reference region selection and the association between the rate of amyloid accumulation over time and the baseline amyloid burden. *Eur J Nucl Med Mol Imaging*. 2017;44(8):1364-1374. doi: 10.1007/s00259-017-3666-8
125. Brendel M, Högenauer M, Delker A, et al. Improved longitudinal [18F]-AV45 amyloid PET by white matter reference and VOI-based partial volume effect correction. *NeuroImage*. 2015;108:450-459. doi: 10.1016/j.neuroimage.2014.11.055
126. Rullmann M, Dukart J, Hoffmann KT, et al. Partial-volume effect correction improves quantitative analysis of 18F-Florbetaben β-Amyloid PET scans. *J Nucl Med Off Publ Soc Nucl Med*. 2016;57(2):198-203. doi: 10.2967/jnumed.115.161893
127. Rullmann M, McLeod A, Grothe MJ, Sabri O, Barthel H, Alzheimer's Disease Neuroimaging Initiative. Reshaping the amyloid buildup curve in Alzheimer Disease? Partial-volume effect correction of longitudinal amyloid PET data. *J Nucl Med Off Publ Soc Nucl Med*. 2020;61(12):1820-1824. doi: 10.2967/jnumed.119.238477
128. Jack Jr CR, Wiste HJ, Weigand SD, et al. Predicting future rates of tau accumulation on PET. *Brain*. 2020;143(10):3136-3150. Published online 2020.
129. Knopman DS, Lundt ES, Therneau TM, et al. Association of initial β-Amyloid levels with subsequent Flortaucipir positron emission tomography changes in persons without cognitive impairment. *JAMA Neurol*. 2021;78(2):217. doi: 10.1001/jamaneurol.2020.3921
130. Villemagne VL, Ong K, Mulligan RS, et al. Amyloid imaging with 18F-Florbetaben in Alzheimer disease and other dementias. *J Nucl Med*. 2011;52(8):1210-1217. doi: 10.2967/jnumed.111.089730
131. Yang J, Hu C, Guo N, et al. Partial volume correction for PET quantification and its impact on brain network in Alzheimer's disease. *Sci Rep*. 2017;7(1):13035. doi: 10.1038/s41598-017-13339-7
132. Schwarz CG, Gunter JL, Lowe VJ, et al. A comparison of partial volume correction techniques for measuring change in serial Amyloid PET SUVR. *J Alzheimers Dis*. 2019;67(1):181-195. doi: 10.3233/JAD-180749
133. Burger C, Goerres G, Schoenes S, Buck A, Lonn A, von Schulthess G. PET attenuation coefficients from CT images: experimental evaluation of the transformation of CT into PET 511-keV attenuation coefficients. *Eur J Nucl Med Mol Imaging*. 2002;29(7):922-927. doi: 10.1007/s00259-002-0796-3
134. Ladefoged CN, Law I, Anazodo U, et al. A multi-centre evaluation of eleven clinically feasible brain PET/MRI attenuation correction techniques using a large cohort of patients. *NeuroImage*. 2017;147:346-359. doi: 10.1016/j.neuroimage.2016.12.010
135. Yin T, Obi T. Generation of attenuation correction factors from time-of-flight PET emission data using high-resolution residual U-net. *Biomed Phys Eng Express*. 2021;7(6):065006. doi: 10.1088/2057-1976/ac21aa
136. Fleisher AS, Joshi AD, Sundell KL, et al. Use of white matter reference regions for detection of change in florbetapir positron emission tomography from completed phase 3 solanezumab trials. *Alzheimers Dement*. 2017;13(10):1117-1124. doi: 10.1016/j.jalz.2017.02.009
137. Chen K, Roontiva A, Thiyyagura P, et al. Improved power for characterizing longitudinal Amyloid-β PET changes and evaluating amyloid-modifying treatments with a cerebral white matter reference region. *J Nucl Med*. 2015;56(4):560-566. doi: 10.2967/jnumed.114.149732
138. Schwarz CG, Senjem ML, Gunter JL, et al. Optimizing PiB-PET SUVR change-over-time measurement by a large-scale analysis of longitudinal reliability, plausibility, separability, and correlation with MMSE. *NeuroImage*. 2017;144:113-127. doi: 10.1016/j.neuroimage.2016.08.056
139. Southekal S, Devous MD, Kennedy I, et al. Flortaucipir F 18 quantitation using parametric estimation of reference signal intensity. *J Nucl Med*. 2018;59(6):944-951. doi: 10.2967/jnumed.117.200006
140. Kameyama M, Ishibash K, Wagatsuma K, Toyohara J, Ishii K. A pitfall of white matter reference regions used in [18F] florbetapir PET: a consideration of kinetics. *Ann Nucl Med*. 2019;33(11):848-854. doi: 10.1007/s12149-019-01397-y
141. Bullich S, Villemagne VL, Catafau AM, et al. Optimal reference region to measure longitudinal Amyloid-β change with ^{18} F-Florbetaben PET. *J Nucl Med*. 2017;58(8):1300-1306. doi: 10.2967/jnumed.116.187351
142. Villemagne VL, The Quest for a Robust and Reliable Reference Region (RR): Exploring RR stability across clinical categories, across Aβ status and across time for five different Aβ radiotracers.
143. Weaver NA, Doeven T, Barkhof F, et al. Cerebral amyloid burden is associated with white matter hyperintensity location in specific posterior white matter regions. *Neurobiol Aging*. 2019;84:225-234. doi: 10.1016/j.neurobiolaging.2019.08.001
144. Roseborough A, Ramirez J, Black SE, Edwards JD. Associations between amyloid β and white matter hyperintensities: a systematic review. *Alzheimers Dement*. 2017;13(10):1154-1167. doi: 10.1016/j.jalz.2017.01.026
145. Moscoso A, Grothe MJ, Schöll M, Alzheimer's Disease Neuroimaging Initiative. Reduced [18F]flortaucipir retention in white matter hyperintensities compared to normal-appearing white matter. *Eur J Nucl Med Mol Imaging*. 2021;48(7):2283-2294. doi: 10.1007/s00259-021-05195-5
146. Yun HJ, Moon SH, Kim HJ, et al. Centiloid method evaluation for amyloid PET of subcortical vascular dementia. *Sci Rep*. 2017;7(1):16322. doi: 10.1038/s41598-017-16236-1
147. Coath W, Modat M, Cardoso MJ, et al. Operationalising the centiloid scale for [^{18}F]Florbetapir PET studies on PET/MR. *Radiology and Imaging*. 2022. doi: 10.1101/2022.02.11.22270590
148. Chincarini A, Sensi F, Rei L. Standardized uptake value ratio-independent evaluation of brain amyloidosis. *J Alzheimers Dis*. 2016;54(4):1437-1457. doi: 10.3233/JAD-160232
149. Leuzy A, Lilja J, Buckley CJ, et al. Derivation and utility of an Aβ-PET pathology accumulation index to estimate Aβ load. *Neurology*;95(21):e2834-e2844. doi: 10.1212/WNL.0000000000011031 Published online October 19, 2020
150. Pegueroles J, Montal V, Bejanin A, et al. AMYQ: an index to standardize quantitative amyloid load across PET tracers. *Alzheimers Dement*. 2021;17(9):1499-1508. doi: 10.1002/alz.12317 Published online April 2, 2021:alz.12317
151. Prosser L, Veale T, Malone IB, Coath W, Fox NC, Cash DM. Amyloid Pattern Similarity Score (AMPSS): a reference region free measure of amyloid PET deposition in Alzheimer's disease. *Alzheimers Dement*. 2020;16(S4):e042673. doi: 10.1002/alz.042673
152. Braak H, Braak E. Neuropathological stageing of Alzheimer-related changes. *Acta Neuropathol (Berl)*. 1991;82(4):239-259. doi: 10.1007/BF00308809
153. Braak H, Alafuzoff I, Arzberger T, Kretzschmar H, Del Tredici K. Staging of Alzheimer disease-associated neurofibrillary pathology using paraffin sections and immunocytochemistry. *Acta Neuropathol (Berl)*. 2006;112(4):389-404. doi: 10.1007/s00401-006-0127-z
154. Pontecorvo MJ, Devous Sr MD, Navitsky M, et al. Relationships between flortaucipir PET tau binding and amyloid burden, clinical diagnosis, age and cognition. *Brain*. 2017;140(3):748-763. doi: 10.1093/brain/aww334
155. Vermeiren C, Motte P, Viot D, et al. The tau positron-emission tomography tracer AV-1451 binds with similar affinities to tau fibrils and monoamine oxidases. *Mov Disord Off J Mov Disord Soc*. 2018;33(2):273-281. doi: 10.1002/mds.27271
156. Wolters EE, Golla SSV, Timmers T, et al. A novel partial volume correction method for accurate quantification of [18F] Flortaucipir in the hippocampus. *EJNMMI Res*. 2018;8(1):79. doi: 10.1186/s13550-018-0432-2
157. Guo T, Brendel M, Grimmer T, Rominger A, Yakushev I. Predicting regional pattern of longitudinal β-Amyloid accumulation by

baseline PET. *J Nucl Med*. 2017;58(4):639-645. doi: 10.2967/jnumed.116.176115
158. Kadir A, Almkvist O, Forsberg A, et al. Dynamic changes in PET amyloid and FDG imaging at different stages of Alzheimer's disease. *Neurobiol Aging*. 2012;33(1):198.e1-198.e14. doi: 10.1016/j.neurobiolaging.2010.06.015
159. Scheinin NM, Aalto S, Koikkalainen J, et al. Follow-up of [11C]PIB uptake and brain volume in patients with Alzheimer disease and controls. *Neurology*. 2009;73(15):1186-1192. doi: 10.1212/WNL.0b013e3181bacf1b
160. Desikan RS, Ségonne F, Fischl B, et al. An automated labeling system for subdividing the human cerebral cortex on MRI scans into gyral based regions of interest. *NeuroImage*. 2006;31(3):968-980. doi: 10.1016/j.neuroimage.2006.01.021
161. Tzourio-Mazoyer N, Landeau B, Papathanassiou D, et al. Automated anatomical labeling of activations in SPM using a macroscopic anatomical parcellation of the MNI MRI single-subject brain. *NeuroImage*. 2002;15(1):273-289. doi: 10.1006/nimg.2001.0978
162. Hammers A, Allom R, Koepp MJ, et al. Three-dimensional maximum probability atlas of the human brain, with particular reference to the temporal lobe. *Hum Brain Mapp*. 2003;19(4):224-247. doi: 10.1002/hbm.10123
163. Brendel M, Sauerbeck J, Greven S, et al. Serotonin selective reuptake inhibitor treatment improves cognition and grey matter atrophy but not amyloid burden during two-year follow-up in mild cognitive impairment and Alzheimer's disease patients with depressive symptoms. *J Alzheimers Dis*. 2018;65(3):793-806. doi: 10.3233/JAD-170387
164. Hansen AK, Parbo P, Ismail R, Østergaard K, Brooks DJ, Borghammer P. Tau Tangles in Parkinson's disease: a 2-year follow-up flortaucipir PET study. *J Parkinsons Dis*. 2020;10(1):161-171. Published online 2019.
165. Schwarz CG, Gunter JL, Ward CP, et al. The Mayo clinic adult life span template: better quantification across the life span. *Alzheimers Dement*. 2017;13(7):P93-P94. doi: 10.1016/j.jalz.2017.06.2396
166. Makris N, Goldstein JM, Kennedy D, et al. Decreased volume of left and total anterior insular lobule in schizophrenia. *Schizophr Res*. 2006;83(2):155-171. doi: 10.1016/j.schres.2005.11.020
167. Lawrence RM, Bridgeford EW, Myers PE, et al. Standardizing human brain parcellations. *Sci Data*. 2021;8(1):78. doi: 10.1038/s41597-021-00849-3
168. SPM12. Accessed April 12, 2021. https://www.fil.ion.ucl.ac.uk/spm/software/spm12/
169. Bourgeat P, Doré V, Doecke J, et al. Non-negative matrix factorisation improves Centiloid robustness in longitudinal studies. *NeuroImage*. 2021;226:117593. doi: 10.1016/j.neuroimage.2020.117593
170. Su Y, Flores S, Wang G, et al. Comparison of Pittsburgh compound B and florbetapir in cross-sectional and longitudinal studies. *Alzheimers Dement Diagn Assess Dis Monit*. 2019;11(1):180-190. doi: 10.1016/j.dadm.2018.12.008
171. Bourgeat P, Doré V, Fripp J, et al. Implementing the centiloid transformation for 11C-PiB and β-amyloid 18F-PET tracers using CapAIBL. *NeuroImage*. 2018;183:387-393. doi: 10.1016/j.neuroimage.2018.08.044
172. Cho SH, Choe YS, Kim HJ, et al. A new Centiloid method for 18F-florbetaben and 18F-flutemetamol PET without conversion to PiB. *Eur J Nucl Med Mol Imaging*. 2020;47(8):1938-1948. doi: 10.1007/s00259-019-04596-x
173. Whittington A, Gunn RN. Amyloid load: a more sensitive biomarker for amyloid imaging. *J Nucl Med*. 2019;60(4):536-540. doi: 10.2967/jnumed.118.210518
174. Whittington A, Sharp DJ, Gunn RN. Spatiotemporal distribution of β-Amyloid in Alzheimer disease is the result of heterogeneous regional carrying capacities. *J Nucl Med*. 2018;59(5):822-827. doi: 10.2967/jnumed.117.194720
175. Lilja J, Leuzy A, Chiotis K, Savitcheva I, Sörensen J, Nordberg A. Spatial normalization of 18F-Flutemetamol PET images using an adaptive principal-component template. *J Nucl Med*. 2019;60(2):285-291. doi: 10.2967/jnumed.118.207811
176. Liu H, Nai YH, Saridin F, et al. Improved amyloid burden quantification with nonspecific estimates using deep learning. *Eur J Nucl Med Mol Imaging*. 2021;48(6):1842-1853. doi: 10.1007/s00259-020-05131-z Published online January 7, 2021
177. Tanaka T, Stephenson MC, Nai YH, et al. Improved quantification of amyloid burden and associated biomarker cut-off points: results from the first amyloid Singaporean cohort with overlapping cerebrovascular disease. *Eur J Nucl Med Mol Imaging*. 2020;47(2):319-331. doi: 10.1007/s00259-019-04642-8
178. Zammit MD, Laymon CM, Betthauser TJ, et al. Amyloid accumulation in Down syndrome measured with amyloid load. *Alzheimers Dement Diagn Assess Dis Monit*. 2020;12(1):e12020. doi: 10.1002/dad2.12020
179. Ashburner J. Symmetric diffeomorphic modeling of longitudinal structural MRI. *Front Neurosci*. 2013;6:197. doi: 10.3389/fnins.2012.00197
180. Ellis S, Reader AJ. Simultaneous maximum a posteriori longitudinal PET image reconstruction. *Phys Med Biol*. 2017;62(17):6963-6979. doi: 10.1088/1361-6560/aa7b49
181. Ellis S, Reader AJ. Penalized maximum likelihood simultaneous longitudinal PET image reconstruction with difference-image priors. *Med Phys*. 2018;45(7):3001-3018. doi: 10.1002/mp.12937
182. Ellis S, Multi-dataset image reconstruction for longitudinal and multi-tracer positron emission tomography. Published online 2019.
183. Tiss A, Joint reconstruction of longitudinal positron emission tomography studies for tau protein imaging. Published online 2019.
184. Kolinger GD, Vállez García D, Willemsen ATM. Amyloid burden quantification depends on PET and MR image processing methodology. *PLOS ONE*. 2021;16(3):e0248122. doi: 10.1371/journal.pone.0248122
185. Farrell ME, Chen X, Rundle MM, Chan MY, Wig GS, Park DC. Regional amyloid accumulation and cognitive decline in initially amyloid-negative adults. *Neurology*. 2018;91(19):e1809-e1821. doi: 10.1212/WNL.0000000000006469
186. Tustison NJ, Holbrook AJ, Avants BB. Longitudinal mapping of cortical thickness measurements: an Alzheimer's disease neuroimaging initiative-based evaluation study. *J Alzheimers Dis*. 2019;71(1):165-183. doi: 10.3233/JAD-190283
187. Leung KK, Ridgway GR, Ourselin S, Fox NC. Consistent multi-time-point brain atrophy estimation from the boundary shift integral. *NeuroImage*. 2012;59(4):3995-4005. doi: 10.1016/j.neuroimage.2011.10.068
188. Fox NC, Ridgway GR, Schott JM. Algorithms, atrophy and Alzheimer's disease: cautionary tales for clinical trials. *NeuroImage*. 2011;57(1):15-18. doi: 10.1016/j.neuroimage.2011.01.077
189. Schwarz CG, Therneau TM, Weigand SD, et al. Selecting software pipelines for change in flortaucipir SUVR: balancing repeatability and group separation. *NeuroImage*. 2021;238:118259. doi: 10.1016/j.neuroimage.2021.118259
190. Minoshima S, Drzezga AE, Barthel H, et al. SNMMI procedure standard/EANM practice guideline for Amyloid PET Imaging of the Brain 1.0. *J Nucl Med*. 2016;57(8):1316-1322. doi: 10.2967/jnumed.116.174615
191. Tian M, Civelek AC, Carrio I, et al. International consensus on the use of tau PET imaging agent 18F-flortaucipir in Alzheimer's disease. *Eur J Nucl Med Mol Imaging*. 2022;49(3):895-904. doi: 10.1007/s00259-021-05673-w
192. Shekari M, Niñerola-Baizán A, Salvadó G, et al. Harmonization of amyloid PET scans minimizes the impact of reconstruction parameters on centiloid values. *Alzheimers Dement*. 2020;16(S4):e045294. doi: 10.1002/alz.045294

193. Joshi A, Koeppe RA, Fessler JA. Reducing between scanner differences in multi-center PET studies. *NeuroImage*. 2009;46(1):154-159. doi: 10.1016/j.neuroimage.2009.01.057
194. Beer JC, Tustison NJ, Cook PA, et al. Longitudinal ComBat: a method for harmonizing longitudinal multi-scanner imaging data. *Neuroscience*. 2020;220:117129. doi: 10.1101/868810
195. Orlhac F, Boughdad S, Philippe C, et al. A Postreconstruction harmonization method for multicenter radiomic studies in PET. *J Nucl Med*. 2018;59(8):1321-1328. doi: 10.2967/jnumed.117.199935
196. Klunk WE, Koeppe RA, Price JC, et al. The Centiloid project: standardizing quantitative amyloid plaque estimation by PET. *Alzheimers Dement J Alzheimers Assoc*. 2015;11(1):1-15.e4. doi: 10.1016/j.jalz.2014.07.003
197. Properzi MJ, Buckley RF, Chhatwal JP, et al. Nonlinear Distributional Mapping (NoDiM) for harmonization across amyloid-PET radiotracers. *NeuroImage*. 2019;186:446-454. doi: 10.1016/j.neuroimage.2018.11.019
198. Su Y, D'Angelo GM, Vlassenko AG, et al. Quantitative Analysis of PiB-PET with FreeSurfer ROIs. *PLOS ONE*. 2013;8(11):e73377. doi: 10.1371/journal.pone.0073377
199. Iaccarino L, R LaJoie, Koeppe R, et al. rPOP: robust PET-only processing of community acquired heterogeneous amyloid-PET data. *NeuroImage*. 2022;246:118775. doi: 10.1016/j.neuroimage.2021.118775
200. Bourgeat P, Doré V, Fripp J, Villemagne V, Rowe C, Salvado O. Computational Analysis of PET by AIBL (CapAIBL): a cloud-based processing pipeline for the quantification of PET images. *J Nucl Med*. 2015;56(supp 3):149-149.

SUPPORTING INFORMATION

Additional supporting information can be found online in the Supporting Information section at the end of this article.

How to cite this article: Bollack A, Pemberton HG, Collij LE, et al. Longitudinal amyloid and tau PET imaging in Alzheimer's disease: A systematic review of methodologies and factors affecting quantification. *Alzheimer's Dement*. 2023;1-21. https://doi.org/10.1002/alz.13158